Lithos 170–171 (2013) 35–53

Contents lists available at SciVerse ScienceDirect

Lithos

journal homepage: www.elsevier.com/locate/lithos

U–Pb dates and trace-element geochemistry of zircon from migmatite, Western Gneiss Region, Norway: Significance for history of partial melting in continental subduction

Stacia M. Gordon [a,*], Donna L. Whitney [b], Christian Teyssier [b], Haakon Fossen [c]

[a] Department of Geological Sciences, University of Nevada, Reno, NV 89557, United States
[b] Department of Earth Sciences, University of Minnesota, Minneapolis, MN 55455, United States
[c] Department of Earth Science, University of Bergen, Bergen, Norway

ARTICLE INFO

Article history:
Received 10 September 2012
Accepted 8 February 2013
Available online 16 February 2013

Keywords:
Partial melting
Eclogite
U–Pb geochronology
Trace elements
Western Gneiss Region

ABSTRACT

The Western Gneiss Region (WGR), Norway, is dominated by migmatitic gneiss that contains inclusions of eclogite, some of which contain evidence for ultrahigh-pressure metamorphism. To evaluate geochemical and age relationships between host migmatite and eclogite, we obtained LA–ICP–MS U–Pb dates and trace-element analyses for zircon from a variety of textural types of leucosome, from layer-parallel to crosscutting. Zircon textures (euhedral, oscillatory- and sector-zone grains) indicate a likely magmatic origin of the leucosomes. Caledonian U–Pb zircon dates from zircon rim and near-rim regions are as old as 410–406 Ma, coeval with previously determined ages of high- and ultrahigh-pressure metamorphism of WGR eclogite. Trace-element analyses obtained simultaneously with U–Pb dates indicate crystallization of zircon under garnet-present conditions in the majority of leucosomes. Other zircons, including those from crosscutting pegmatite, yield younger ages (as young as 385 Ma), coinciding with dates determined for amphibolite-facies retrogression of eclogite; trace-element analyses suggest that these zircons grew under plagioclase-present (garnet-absent) conditions. Combined age and trace-element data for leucosome zircons record the transition from high-pressure (garnet-present, plagioclase-absent) crystallization to lower-pressure (plagioclase-present) crystallization. If the euhedral zircons that yield ages coeval with peak or near-peak UHP metamorphism represent crystallization from anatectic leucosomes, these results, combined with field and petrographic observations of eclogite–migmatite relationships, are consistent with the presence of partially molten crust in at least part of the WGR during continental subduction. The decreased viscosity and increased buoyancy and strain weakening associated with partial melting may have assisted the rapid ascent of rocks from mantle to crustal depths.

1. Introduction

Exhumed ultrahigh-pressure (UHP) terranes document the subduction of crustal material to mantle depths and its return to the Earth's surface (e.g., Chopin, 1984; Hacker, 2006; Liou et al., 2000; Rubatto and Hermann, 2001). One of the main modes of occurrence of UHP rocks is as eclogite (metabasalt and metagabbro) inclusions in migmatitic gneiss (Group B eclogites of Coleman et al., 1965). Although evidence for UHP metamorphism in the gneiss is rare (Dobrzhinetskaya et al., 1995), it is likely that both eclogite and gneiss were metamorphosed at UHP conditions (e.g., Cuthbert et al., 2000; Hacker, 2006; Wain, 1997). However, the relationship of migmatization of the gneiss—specifically, partial melting—to UHP metamorphism (Labrousse et al., 2011) is not well established.

Important questions are whether partial melting of the gneiss occurred during an orogenic episode that pre-dated UHP eclogite metamorphism (and therefore the gneiss remained at subsolidus conditions during UHP metamorphism) or whether migmatization occurred during the same metamorphic event that produced the UHP eclogite. In the latter case, it is important to determine the conditions of migmatization, and in particular, whether partial melting occurred at high or ultrahigh pressures and/or at much lower pressures related to decompression to mid-crustal (amphibolite-facies) levels (Fig. 1).

These questions are significant because the presence or absence of partial melt during continental subduction affects the rheology of the subducted crust, and therefore the mechanism and rate of exhumation. Field, experimental, and modeling studies suggest that partial melting may occur under the UHP conditions of continental subduction (Auzanneau et al., 2006; Brueckner, 2009; Hermann, 2002; Lang and Gilotti, 2007; Liu et al., 2012; Wallis et al., 2005; Whitney et al., 2004, 2009; Zhang et al., 2009). If present, partial melt (with melt fraction > 10–15%) will dramatically decrease viscosity (Rosenberg and

* Corresponding author.
E-mail address: staciag@unr.edu (S.M. Gordon).

0024-4937/$ – see front matter © 2013 Elsevier B.V. All rights reserved.
http://dx.doi.org/10.1016/j.lithos.2013.02.003

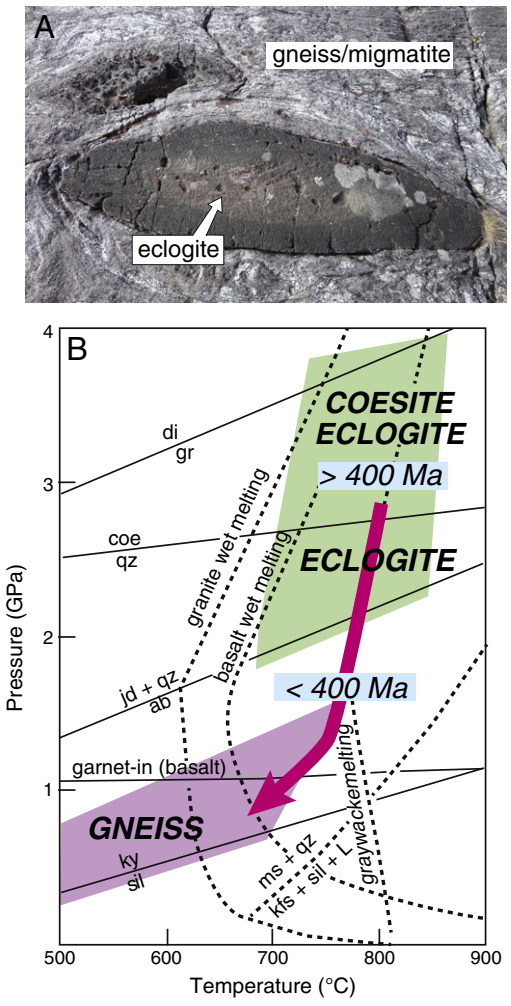

Fig. 1. (A) Outcrop photographs showing meter-scale eclogite lens in migmatitic gneiss, northern UHP domain (WGR, Norway). (B) P–T diagram showing the relationship of WGR metamorphic conditions recorded by eclogite and gneiss and various solidi for meta-igneous and metasedimentary rocks (solidi from Prouteau et al., 2001; Auzanneau et al., 2006; Labrousse et al., 2011; and references therein). Note that although both eclogite and gneiss likely experienced UHP conditions, the gneiss equilibrated at much lower P–T conditions during decompression. Timing of "peak" UHP and lower-P metamorphism from Hacker et al. (2010) and references therein.

Handy, 2005), thus changing the overall deformation regime of the subducted crustal material and potentially of the orogen developing in the overriding plate.

In the Western Gneiss Region (WGR) of Norway (Fig. 2), evidence for (U)HP metamorphism is primarily preserved in eclogite included in gneiss (Carswell et al., 1999; Smith, 1984), although microdiamond has been reported from metapelitic gneiss in the region (Dobrzhinetskaya et al., 1995). Owing to its spectacular exposure and preservation of UHP metamorphism, WGR eclogite has been the focus of much petrological, geochemical, and geochronological research to determine the pressure–temperature–time (P–T–t) history of metamorphism. Studies using a variety of isotopic systems have thoroughly documented Late Silurian to Early Devonian (~425–400 Ma) metamorphism of the Scandian phase of the Caledonian orogeny (Carswell et al., 2003a; Krogh et al., 2011; Kylander-Clark et al., 2007, 2008; Root et al., 2004; Walsh et al., 2007). Studies of gneiss hosting eclogite inclusions in the WGR have documented Precambrian metamorphism (Gorbatschev, 1985; Kullerud et al., 1986; Skår and Pedersen, 2003; Tucker et al., 1990), as well as Caledonian ages for some migmatitic gneiss and pegmatite (Krogh et al., 2004, 2011; Kylander-Clark et al., 2008; Schärer and Labrousse, 2003; this study).

The record of Caledonian migmatization is of particular interest for evaluating relationships between host migmatite and eclogite inclusions in the WGR. Comparison of the P–T paths of Caledonian eclogite with melting and dehydration reactions (Fig. 1), and investigation of the composition and textural locations of leucosomes (Fig. 3) suggests that partial melting may have begun at the high-pressure conditions recorded by WGR eclogite (Labrousse et al., 2011). High-pressure migmatization is further supported by isotopic and inclusion studies that indicate interaction of eclogite and peridotite with the surrounding migmatitic gneiss at near-peak conditions (Griffin and Brueckner, 1985; Vrijmoed et al., 2009).

In this paper, we contribute to ongoing discussion of the occurrence, conditions, and consequences of partial melting in continental subduction by presenting new geochronological and geochemical data for migmatites that host (U)HP eclogite in the WGR. Migmatites in the WGR exhibit a range of textures that may indicate the involvement of melt during metamorphism and deformation (Fig. 3), but the timing of migmatization has not previously been systematically determined for different textural varieties of crystallized melt bodies spatially associated with eclogite. Some previous geochronology studies have focused on texturally late leucosomes (e.g., Krogh et al., 2011) or have dated leucosome minerals using techniques that yield cooling ages, not crystallization ages (e.g., U–Pb titanite; Schärer and Labrousse, 2003). In this study, we focused on a range of migmatite textures, from layer-parallel leucosomes to crosscutting dikes, in order to evaluate migmatite–eclogite relationships from (U)HP to lower-P conditions.

2. Brief overview of the Western Gneiss Region

The WGR is one of the largest and best-exposed ultrahigh-pressure terranes on Earth. UHP conditions are primarily recorded in eclogite pods within migmatite that records polyphase metamorphism (Tucker et al., 1990). The WGR has been the site of many studies of UHP metamorphism, including investigations that focused on the petrology of crustal and mantle rocks (Butler et al., 2013; Carswell and van Roermund, 2005; Carswell et al., 1999, 2003b; Cuthbert et al., 2000; Dobrzhinetskaya et al., 1995; Scambelluri et al., 2008; Smith, 1984; van Roermund et al., 2001, 2002; Vrijmoed et al., 2006; Wain et al., 2000, 2001), the timing of (U)HP metamorphism and exhumation (Carswell et al., 2003a, 2006; Hacker, 2007; Hollocher et al., 2007; Krogh et al., 2011; Kylander-Clark et al., 2007, 2008; Root et al., 2004; Spengler et al., 2009; Walsh et al., 2007), and the structural history and regional tectonic evolution (Brueckner and van Roermund, 2004; Engvik et al., 2007; Foreman et al., 2005; Fossen, 2010; Hacker and Gans, 2005; Hacker et al., 2003, 2010; Johnston et al., 2007; Kylander-Clark et al., 2009; Root et al., 2005; Terry and Robinson, 2003, 2004; Terry et al., 2000a, 2000b; Walsh and Hacker, 2004).

UHP rocks are exposed in three domains in the WGR: south, central, and north (Fig. 2). Many workers have proposed a SE to NW increase in P–T conditions, from 700 °C, ~2.8 GPa in the southern UHP domain to 850 °C, 3.2–3.6 GPa in the north (Cuthbert et al., 2000; Hacker, 2006; Ravna and Terry, 2004). Moreover, maximum P–T conditions may have been as high as 7 GPa and 1000 °C, based on the occurrence of majoritic garnet in websterite (Scambelluri et al., 2008). Leucosomes containing hornblende and Caledonian titanite increase in abundance from southeast to northwest, and the greatest melt fractions in migmatite occur in the northwestern WGR, consistent with the proposal that these rocks achieved the highest Caledonian P–T conditions (Hacker et al., 2010). A possible exception to this trend is a southern-domain eclogite in which microdiamond inclusions in garnet have been identified, indicating a minimum pressure of 3.5 GPa (Smith and Godard, 2013).

Previous WGR geochronology studies have established the timing of Caledonian (Scandian) UHP metamorphism at 425–400 Ma, and have determined the timing (400–385 Ma) of a lower pressure, amphibolite-facies (1.5–0.5 GPa) overprint at similar or slightly higher

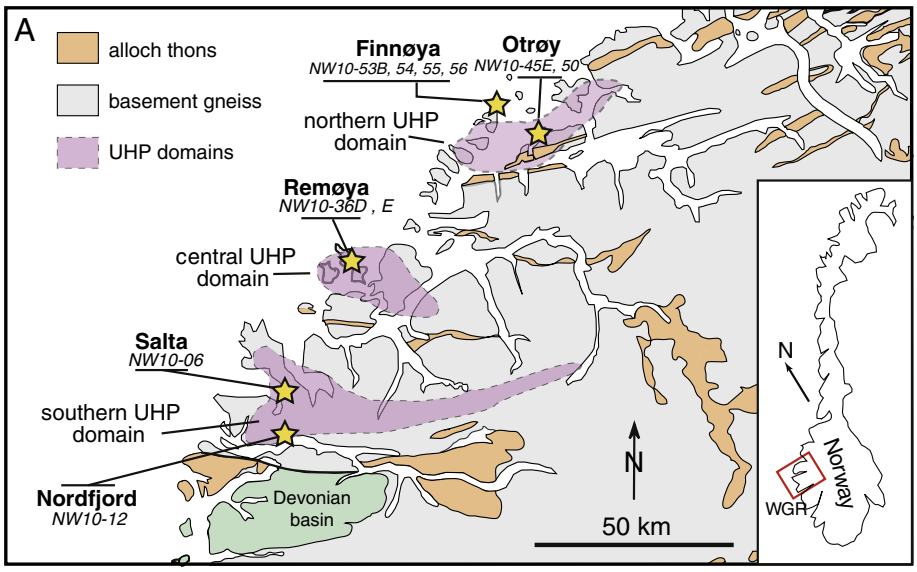

Fig. 2. (A) Simplified geological map of the Western Gneiss Region, Norway, showing sample localities (marked by the yellow stars) within the three UHP domains. (For interpretation of the references to color in this figure legend, the reader is referred to the web version of this article.)
Modified from Kylander-Clark et al. (2008).

temperatures than those of UHP metamorphism (Krogh et al., 2011; Kylander-Clark et al., 2007, 2008; Terry et al., 2000a; Walsh et al., 2007). One of the few geochronology studies of WGR migmatite that hosts eclogite obtained a U–Pb rutile age of 389 ± 7 Ma for eclogite and a U–Pb cooling age of 375 ± 6 Ma for titanite and K-feldspar in host migmatite (Schärer and Labrousse, 2003). Similarly, a regional U–Pb titanite study of orthogneiss revealed a cooling age range of 393–389 Ma, interpreted as dating the timing of the amphibolite-facies overprint (Kylander-Clark et al., 2008). Texturally late, undeformed pegmatite dikes in the northern UHP domain contain zircons that yield crystallization ages of ca. 395 Ma; these dates were interpreted as revealing the timing of exhumation to ~30 km depth (Krogh et al., 2011).

3. Methods and samples

To assess the timing of migmatization relative to eclogite metamorphism, we collected tonalitic and granodioritic leucosomes that represent a variety of textures and geographic locations in the WGR (Figs. 2, 3). We separated zircon from each leucosome sample using standard mineral-separation techniques and then prepared grain mounts and examined zircon grains using cathodoluminescence (CL) imaging to characterize internal structure (Fig. 4). The U–Th–Pb analyses of zircon were acquired by laser-ablation inductively coupled plasma mass spectrometry (LA–ICP–MS) at the University of California-Santa Barbara. Analyses were performed in "split-stream" mode, allowing the simultaneous collection of isotopic data and trace-element abundance for each analyzed zircon spot (see supplementary material online for detailed methodology; Kylander-Clark et al., in press).

In this paper, we focus on two sites in the southern domain (Salta, Nordfjord), one site (Remøya) in the central domain, and two sites (Otrøy, Finnøya) in or near the northern UHP domain (Fig. 2).

We examined zircon in different textural types of leucosome (Fig. 3):

(1) layer-parallel leucosome (Finnøya, Otrøy, Salta; Fig. 3A);
(2) eclogite-margin leucosome (Remøya, Nordfjord, Otrøy; Fig. 3B);
(3) inter-boudin leucosome (Finnøya; Fig. 3C); and
(4) cross-cutting, pegmatitic dike (Finnøya (Fig. 3D).

4. Geochronology results

Zircons were extracted from a total of eight leucosome bodies and one crosscutting (but deformed) pegmatite dike (Fig. 2). CL images reveal that most of the zircons have distinct interior and rim zoning (Fig. 4), although some grains consist entirely of one textural/compositional domain. The rims were mainly targeted for the analyses, and typically have oscillatory and/or sector zoning (Fig. 4). We interpret the oscillatory and/or sector zoning and crystal shape to indicate that the rims may have crystallized from melt (e.g., Hoskin and Schaltegger, 2003). Interiors commonly yielded Proterozoic dates, whereas the majority of the analyzed rims revealed dates on individual spots in the range of 410–390 Ma (Fig. 5, S1; Table 1).

The samples are presented by outcrop-scale textural type of leucosome: 1) layer-parallel leucosome; 2) eclogite-margin leucosome; 3) inter-boudin leucosome; and 4) a cross-cutting pegmatite. For samples in which a single population of dates is present, concordia or weighted-mean 207-corrected $^{206}Pb/^{238}U$ dates were calculated using Isoplot v3.00 (Ludwig, 2003). For samples in which there is more scatter in the results, we report the individual spot 207-corrected date results (calculated using Isoplot v3.00) and 2-sigma error (Fig. 5, Table 1). The Th/U ratios for the zircons were also measured during the U–Pb analyses. For all the Scandian zircons extracted from the variety of leucosomes, the Th/U ratios are uniformly low, <0.04 (Table 1). Although such low values are commonly interpreted to indicate a metamorphic origin, many zircons that formed during crystallization of melt bodies yield very low Th/U values (e.g., Gordon et al., 2010).

4.1. Layer-parallel leucosomes

From the southern UHP domain, a strongly deformed layer-parallel granitic leucosome (NW10-06) was collected from within a ~50 m wide shear zone exposed on the coast at Salta (Fig. 2). The majority of zircons obtained from this sample reveal interior and rim zoning in the CL images (Fig. 4A). This layer-parallel leucosome yielded only discordant Precambrian $^{207}Pb/^{206}Pb$ rim dates of 919 to 1659 Ma (n = 20; Fig. S1A).

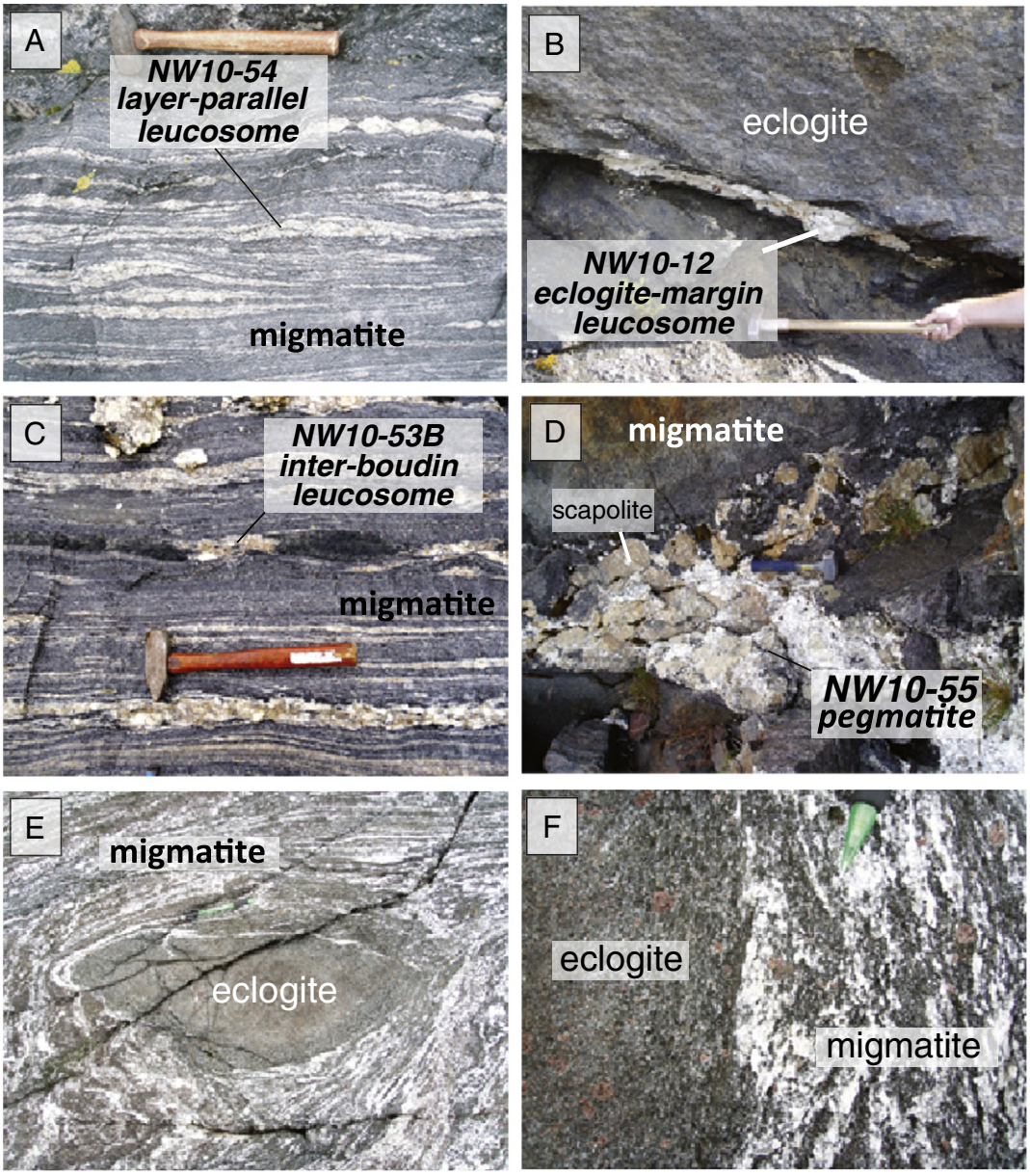

Fig. 3. Field photos of various types of melt phases exposed throughout the WGR: (A) eclogite-margin leucosome, NW10-12, Nordfjord; and (B) inter-boudin leucosome, NW10-53B, Finnøya; (C) layer-parallel leucosome, NW10-54, Finnøya; (D) pegmatite, NW10-55, Finnøya; and (E) and (F) transition from eclogite to migmatite (Otrøy). The migmatite contains garnet and clinopyroxene (typically rimmed by hornblende) with the same composition as those minerals in the eclogite.

From the northern UHP domain, several layer-parallel leucosome samples were collected. Zircons were extracted from a granitic leucosome (NW10-50) on the northern side of Otrøy (Fig. 2). The leucosome is ~5 cm thick and occurs within a mylonitic zone of the migmatitic gneiss. CL images of zircons reveal oscillatory zoning to more complex interior–rim relationships (Fig. 4B). Seventy-two zircon rims were targeted for analyses. Many yielded Precambrian ages, with a mix of concordant and discordant $^{207}Pb/^{206}Pb$ dates ranging from 734 to 1861 Ma (Fig. S1B).

At the Finnøya northern UHP domain locality (Fig. 2), a sample of fine-grained, layer-parallel, garnet-bearing granodioritic leucosome (Fig. 3A; NW10-54) was collected for geochronometric analyses. Some of the zircons from NW10-54 have interior/rim zoning, and the rims reveal oscillatory zoning (Fig. 4C). Ten zircon analyses yielded a range of 207-corrected $^{206}Pb/^{238}U$ dates: 409 ± 8 Ma to 393 ± 9 Ma (Table 1), yielding a weighted-mean age of 401 ± 3 Ma (MSWD = 1.4, n = 16). A few zircon rims yielded older discordant 207-corrected $^{206}Pb/^{238}U$ dates, with results of 417 Ma, 431 Ma, and 445 Ma. Four analyses of the zircon interiors yielded older discordant $^{207}Pb/^{206}Pb$ dates of 1434–1638 Ma. Using the results from the rims and interiors yields an upper-intercept age of 1688 ± 29 Ma and a lower-intercept age of 399 ± 4 Ma (MSWD = 4, n = 23; Fig. 5A).

Cathodoluminescence images of fifteen zircon grains from a coarser-grained, layer-parallel granodioritic leucosome from the same outcrop (NW10-56) show distinct rims that yielded a weighted mean 207-corrected age of 405 ± 2 Ma (MSWD = 1.1; Fig. 4D). Like NW10-54, the Scandian zircons revealed some scatter, with individual 207-corrected dates ranging from 420 ± 8 Ma to 398 ± 7 Ma. Three older discordant $^{207}Pb/^{206}Pb$ dates were obtained from the rims: 1474 Ma, 1517 Ma, and 1648 Ma (Table 1). Analyses of six zircon cores revealed mostly Scandian 207-corrected dates (430–401 Ma; n = 4), and two older discordant $^{207}Pb/^{206}Pb$ dates of 1534 Ma and 1557 Ma. Using the results from the rims and interiors yields an upper-intercept age of 1675 ± 21 Ma and a lower-intercept age of 403 ± 3 Ma (MSWD =

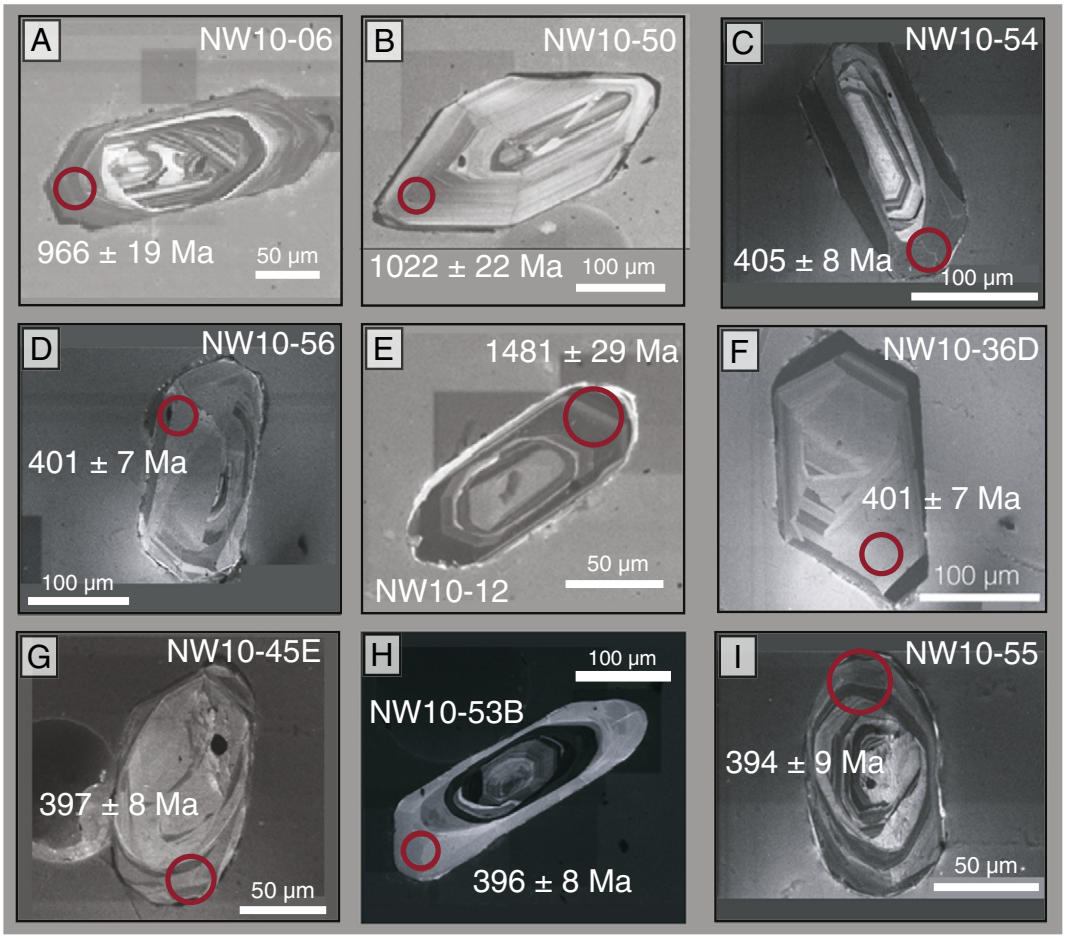

Fig. 4. Representative CL images from the leucosomes and pegmatite: (A) layer-parallel leucosome, NW10-12, Nordfjord; (B) layer-parallel leucosome, NW10-06, Salta; (C) eclogite-margin leucosome, NW10-36D, Remøya; (D) layer-parallel leucosome, NW10-50, Otrøy; (E) eclogite-margin leucosome, NW10-45E, Otrøy; (F) layer-parallel leucosome, NW10-54, Finnøya; (G) inter-boudin leucosome, NW10-53B, Finnøya; (H) layer-parallel leucosome, NW10-56, Finnøya; and (I) pegmatite, NW10-55, Finnøya.

2.3, n = 25; Fig. 5B). Previous work on eclogite in the general vicinity of Finnøya yielded dates of 410 ± 16 Ma (garnet–clinopyroxene–whole rock Sm–Nd isochron; Mørk and Mearns, 1986), and 412 ± 1 Ma, 410 ± 1 Ma and 408 ± 1 Ma (U–Pb zircon, Krogh et al., 2004).

4.2. Eclogite-margin leucosome

From the southern UHP domain, a coarse-grained granodioritic leucosome (NW10-12) containing tourmaline was collected from the margin of an eclogite exposed near Kroken, along the northern side of Nordfjord (Figs. 2, 3B). Most of the dated zircons have a rounded morphology. CL images reveal interior and rim zoning, and the rims exhibit oscillatory and/or sector zoning (Fig. 4E). Analyses targeting ten rims yielded discordant Precambrian $^{207}Pb/^{206}Pb$ dates ranging from 1101 to 1704 Ma (Fig. S1C).

Two leucosomes exposed along margins of different eclogite pods were collected from the northern part of Remøya in the central UHP domain (Fig. 2). Zircons with distinct interior and rim relationships were extracted and imaged from a medium-grained granodioritic leucosome (sample NW10-36D); both interior and rim regions of zircon display oscillatory zoning (Fig. 4F). Most zircon rims yielded Caledonian 207-corrected dates, ranging from 409 ± 8 Ma to 390 ± 8 Ma (n = 16; Fig. 5C). Four additional zircon rims yielded older discordant $^{206}Pb/^{238}U$ dates of 430 Ma, 443 Ma, and 637 Ma, and a $^{207}Pb/^{206}Pb$ date of 1604 Ma (Table 1). The interiors of six zircons that yielded Scandian rim dates were also ablated. These also yielded Scandian dates, with two older grains (426 Ma, 420 Ma) and the rest similar to the younger end of the rim population (397 Ma to 388 Ma; Table 1).

A sheet-like body of granodioritic leucosome was also collected from an eclogite-boudin margin (NW10-36E) from the northern part of Remøya (Fig. 2). Of the twenty-two zircon rims analyzed, only one yielded a Scandian date (397 Ma). The rest of the zircon rims yielded discordant dates mainly > 900 Ma (Table 1; Fig. 4E; S1D). UHP metamorphism in this area is interpreted to have occurred at 398 ± 6 Ma based on Sm–Nd analysis of garnet in eclogite (Kylander-Clark et al., 2007).

From the northern UHP domain, zircons were extracted from a medium-grained granodioritic leucosome (NW10-45E), collected from the pressure shadow of one of many meter-scale, elongate eclogite lenses in the Otrøy outcrop at Tangen (Fig. 2). CL images reveal that most zircons are zoned (Fig. 4G). Zircons from this leucosome revealed Caledonian 207-corrected dates that range from 404 ± 8 Ma to 391 ± 8 (n = 8; Fig. 5D). Five additional analyzed zircon rims yielded older discordant dates: 601 Ma ($^{206}Pb/^{238}U$ date) to 1493 Ma ($^{207}Pb/^{206}Pb$ date) (Table 1); these grains typically have a more rounded morphology. The Caledonian U–Pb dates from this leucosomes overlap with ages from an eclogite interpreted as dating the timing of UHP metamorphism on Otrøy; e.g. a $^{206}Pb/^{238}U$ zircon date of 405 ± 1 Ma (Krogh et al., 2011).

4.3. Inter-boudin leucosome

Zircon grains were extracted from another garnet-bearing granitic leucosome (NW10-53B) from the northern Finnøya UHP domain

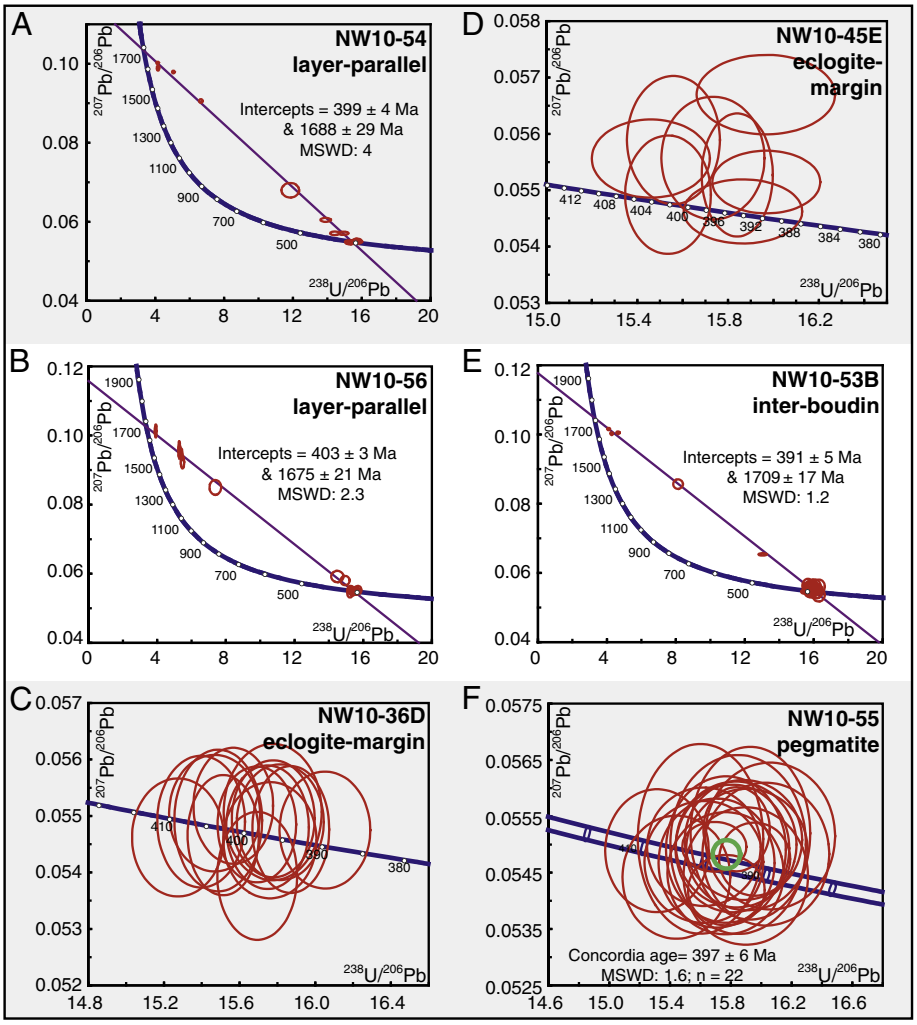

Fig. 5. Concordia diagrams revealing the U–Pb Scandian zircon results for samples: (A) eclogite-margin leucosome, NW10-36D, Remøya; (B) eclogite-margin leucosome, NW10-45E, Otrøy; (C) layer-parallel leucosome, NW10-54, Finnøya; (D) inter-boudin leucosome, NW10-53B, Finnøya; (E) layer-parallel leucosome, NW10-56, Finnøya; and (F) pegmatite, NW10-55, Finnøya. Green ellipse in F represents the concordia age. (For interpretation of the references to color in this figure legend, the reader is referred to the web version of this article.)

locality, but in contrast to the layer-parallel NW10-54 leucosome, this leucosome occurs in the neck of small mafic boudins (Fig. 3C). Some zircon grains extracted from this leucosome show distinct interior and rim zoning relationships, whereas other grains appear to have a single growth event characterized by oscillatory zoning (Fig. 4H). Twenty-nine zircon rims yielded a weighted-mean 207-corrected date of 393 ± 2 Ma (MSWD = 1.2; individual zircons range from 382 ± 9 to 401 ± 9 Ma; Table 1). Five additional zircon rims revealed discordant results (Table 1). Using the results from all the rims yields an upper-intercept age of 1709 ± 17 Ma and a lower-intercept age of 391 ± 5 Ma (MSWD = 1.2, n = 34; Fig. 5E).

4.4. Pegmatite

A scapolite- and garnet-bearing granitic pegmatite (NW10-55) cuts across the gneiss at the Finnøya outcrop but also experienced Scandian deformation (Fig. 3D). As seen in CL images, zircons from this pegmatite have oscillatory zoning and show a single growth event (Fig. 4I). All zircons yielded Scandian dates, with 207-corrected dates ranging from 408 ± 7 Ma to 389 ± 8 Ma (Fig. 5F). A weighted-mean $^{206}Pb/^{238}U$ age of 396 ± 2 Ma (MSWD = 1.2, n = 22) was derived from these dates.

5. Trace-element analysis of zircon rims: REE

Trace-element analyses acquired from zircon simultaneously with the U–Th–Pb isotopic ratios (Fig. 6, Table 2) allow evaluation of the geochemical context of zircon crystallization in the leucosomes. A signature of HP crystallization of zircon is a flat heavy rare earth element (HREE) pattern and the absence of a Eu anomaly (e.g., Rubatto, 2002), although the Eu anomaly may be controlled by other Ca-bearing minerals in the sample, such as plagioclase. For most of the Scandian zircons analyzed, measurements of the light rare earth elements (LREE) were at background levels. Because our focus was on Scandian migmatization, we present trace-element analyses only for central and northern domain samples.

5.1. Layer-parallel leucosomes

Zircon from Finnøya leucosomes revealed a wide spectrum of REE patterns. Zircon from NW10-54, a layer-parallel leucosome, yields flat and consistent HREE patterns ($Lu_n/Dy_n = 1–2$) and slightly negative to positive Eu anomalies ($Eu^* = 0.06$ to -0.21) for eight Scandian zircons (Fig. 6A). In comparison, zircons from another layer-parallel leucosome (NW10-56) at the same outcrop have the most varied

trace-element patterns analyzed (Fig. 6B). For example, one of the 408 Ma zircon grains yields an enriched HREE pattern ($Lu_n/Dy_n = 9$). The remaining ten grains reveal a continuum with Lu_n/Dy_n values ranging from 3.5 to 0.5 (Fig. 6B). The 408 Ma zircon with the steepest HREE slope has a negative Eu anomaly of −0.17; the others have positive anomalies (0.01 to 0.36; Fig. 6D).

5.2. Eclogite-margin leucosome

The eclogite-margin sample from Remøya (NW10-36D) yielded two populations of zircon with distinct REE patterns (Fig. 6C). Both populations have a negative Eu anomaly (where measurable, $Eu^* = -0.51$ to −0.12) and a steep, positive HREE pattern ($Lu_n/Dy_n =$ 10–40; avg = 22). There is no age correlation between the two REE populations (Fig. 6C).

Zircon from the eclogite-margin leucosome from Otrøy (NW10-45E) shows a wide variation in REE concentrations. Four of the eight analyzed zircon rims have steep HREE profiles ($Lu_n/Dy_n = 21$–178), whereas the other four have higher concentrations of the middle rare earth elements (MREE), resulting in a gentler HREE slope ($Lu_n/Dy_n = 8$–11; Fig. 6D). The Otrøy zircons yielded positive to negative Eu anomalies, ranging from 0.24 to −0.63 (Fig. 6D).

5.3. Inter-boudin leucosome/pegmatite

The two youngest and texturally late inter-boudin neck leucosome (NW10-53B) and pegmatite (NW10-55) yield similar REE profiles: moderately steep HREE patterns and mostly negative Eu anomalies (Fig. 6E,F). For NW10-53B, the Lu_n/Dy_n values range from 7 to 3 and Eu^* from −0.93 to −0.02; two grains revealed positive Eu anomalies of 0.02 and 0.12 (Fig. 6E). In comparison, NW10-55 zircons yielded Lu_n/Dy_n values of 6–2 and Eu^* of −0.40 to −0.01, with two grains also revealing positive Eu^* of 0.02 and 0.09 (Fig. 6F).

6. Major and trace-element leucosome geochemistry

Major- and trace-element abundances were determined for representative whole-rock specimens of the leucosomes. Analyses were conducted by the Geoanalytical Laboratory at Washington State University. Major, minor, and trace-element data were analyzed by X-ray fluorescence (XRF), and trace elements were also analyzed by ICPMS (Table 3; Figs. 7, S2, S3). In all figures, the samples are keyed by their textural type. All textural varieties are represented except for the inter-boudin leucosome (NW10-53B) because insufficient sample was available for bulk analysis.

Overall, the leucosome bodies have relatively high but variable SiO_2, ranging from 62.9 to 75.0 wt.%. The concentrations of Al_2O_3, ($Na_2O + CaO$), and ($FeO^* + MgO + TiO_2$) mainly decrease, and K_2O shows no systematic change with increasing SiO_2 (Fig. S1). For the majority of the samples, V decreases systemically, Rb/Sr increases, and Zr and Ba do not show a systematic change with increasing SiO_2 (Fig. S2).

The REE patterns are distinct for several of the leucosomes (Fig. 7). Sample NW10-12, an eclogite-margin leucosome from the southern UHP domain, reveals very low concentrations of all REE, in particular the HREE. The scapolite-rich pegmatite (NW10-55) from the northern UHP domain also yields a distinct REE pattern: low in the LREE, no Eu anomaly, and a steady increasing slope in the MREE and HREE that result in a La_n/Yb_n value of 0.4. In comparison, a leucosome that yielded Proterozoic dates (NW10-50) has a high La_n/Yb_n value of 49. The remaining leucosome bodies exhibit intermediate REE patterns, with an overall decreasing slope from the LREE to the HREE ($La_n/Yb_n = 6$–19). Eclogite-margin leucosomes (NW10-06, NW10-36E, and NW10-45E) reveal distinct positive Eu anomalies (0.19, 0.47, and 0.21, respectively), whereas leucosomes NW10-36D, NW10-50, and NW10-54 have slight negative Eu anomalies (−0.14, −0.08 and −0.02, respectively; Fig. 7).

7. Discussion

7.1. Coeval leucosome crystallization and (U)HP metamorphism?

The majority of the analyzed leucosomes have Proterozoic upper-intercept ages (~1710–1675 Ma) that were primarily obtained from zircon interiors (Table 1). These ages overlap with uncertainty with the 1686–1650 Ma crystallization of WGR granitoids, and previous studies have suggested that most of the WGR migmatite also formed during this time (Gorbatschev, 1985; Kullerud et al., 1986; Skår and Pedersen, 2003; Tucker et al., 1990). We reevaluate this interpretation in light of our new results.

The leucosomes exposed throughout the WGR are present in a variety of structural and textural sites, suggesting early to late crystallization relative to peak UHP metamorphism, as well as a variety of compositions, from trondhjemitic to granitic (Labrousse et al., 2011). In the WGR, leucosomes were derived from a variety of protoliths, including granite and metasedimentary rocks, but field and petrographic observations from the central and northern domain sites in our study are consistent with derivation of migmatite from eclogite (Fig. 3E,F). The migmatitic gneiss analyzed from these sites is a mafic gneiss dominated by hornblende + plagioclase + quartz + biotite, and contains relict clinopyroxene (rimmed by hornblende) and garnet (Fig. 3E,F). Labrousse et al. (2011) also suggested that tonalitic leucosome was derived from eclogite that had partially melted, as the WGR P–T conditions are suitable for water-saturated basalt melting conditions (e.g., Prouteau et al., 2001; Fig. 1). The Scandian leucosomes studied here crystallized at garnet-present conditions (bulk rock $La_n/Yb_n =$ 0–19; Fig. 7; Table 3), consistent with this idea.

The geochronology results reveal that a variety of leucosome textures, from layer-parallel leucosomes to crosscutting dikes, and compositions, from tonalitic to granitic, yield Scandian ages for zircon rims from the central and northern UHP domains (Fig. 5; Table 1). In some cases, for example the layer-parallel leucosome NW10-56 from Finnøya, the zircons reveal a wide range of Scandian dates and geochemical characteristics, suggesting that the Scandian UHP metamorphism and subsequent decompression did not affect every zircon crystal in the same manner within the sample, consistent with other studies of the behavior of zircon in metamorphic systems (e.g., Vorhies et al., 2013).

Southern domain zircons from this study yielded only Proterozoic ages, even in leucosomes that are clearly texturally later than eclogite with Scandian metamorphic ages (Table 1). This is consistent with other findings, in which mainly Proterozoic U–Pb dates were determined for titanite and rutile from pegmatite, leucosome, and gneiss in the western part of the southern UHP domain (Kylander-Clark et al., 2008; Spencer et al., in press). Possible explanations for these results are that zircon (and other accessory minerals) in the southern domain did not readily grow or recrystallize during Scandian metamorphism or that Scandian rims grew but are too narrow to analyze using the LA–ICP–MS technique on grain mounts. In other studies, zircon rim growth during crystallization in a leucosome or high-grade metamorphic rock can only be detected by depth profiling and not by spot analysis of polished crystals (e.g., Gordon et al., 2009; Vorhies et al., 2013). It is also important to note that Beyer et al. (2012) reported Caledonian dates (ca. 400 Ma) from detrital zircons extracted from drainage systems collected just north of Nordfjord and therefore likely derived from rocks exposed in the southern UHP domain. Although the source rocks are not known, it is possible that this study indicates the presence of Scandian zircons from gneiss in the region.

It is important to evaluate whether zircon rim growth occurred at subsolidus conditions during Scandian metamorphism or whether

Table 1
U–Th–Pb isotopic data for zircon from Western Gneiss Region crystallized melt.

Sample, grain number*	$^{207}Pb/^{235}U$	±2σ%	$^{206}Pb/^{238}U$	±2σ%	Error correlation	$^{238}U/^{206}Pb$	±2σ%	$^{207}Pb/^{206}Pb$	±2σ%	Error correlation	$^{208}Pb/^{232}Th$	±2σ%	207-corrected age*	Error	$^{206}Pb/^{238}U$ date (Ma)	±2σ abs	$^{207}Pb/^{235}U$ date (Ma)	±2σ abs	$^{207}Pb/^{206}Pb$ date (Ma)	±2σ abs	Approx. U (ppm)	Approx. Th (ppm)	Th/U
NW10-06, layer-parallel leucosome (*UTM*: *308822, 6882324*)																							
NW10_06_1	1.335	0.016	0.1387	0.0016	0.97	7.21	0.08	0.0697	0.0002	−0.06	0.051	0.003	830.4	15.3	837.3	8.8	861.6	7.0	919.2	2.5	627.2	11.8	0.02
NW10_06_2	3.165	0.037	0.2385	0.0029	0.98	4.19	0.05	0.0960	0.0002	0.16	0.068	0.001	1355.9	26.1	1379.6	15.0	1447.4	9.0	1548.2	3.4	745.1	39.3	0.05
NW10_06_4	1.591	0.023	0.1589	0.0022	0.99	6.29	0.09	0.0724	0.0002	−0.11	0.052	0.001	942.5	19.1	950.4	12.4	965.2	9.1	996.3	2.1	965.6	28.1	0.03
NW10_06_5	1.579	0.023	0.1580	0.0022	0.99	6.33	0.09	0.0720	0.0002	−0.05	0.048	0.001	937.1	19.0	945.1	12.1	961.6	8.7	986.4	2.5	672.1	37.7	0.06
NW10_06_6	3.576	0.036	0.2538	0.0026	0.98	3.94	0.04	0.1019	0.0002	0.17	0.069	0.001	1429.1	26.0	1457.5	13.5	1545.7	8.1	1658.7	3.5	968.1	189.9	0.20
NW10_06_7	1.600	0.021	0.1601	0.0021	0.99	6.25	0.08	0.0721	0.0001	−0.03	0.048	0.001	950.9	18.8	956.9	11.5	969.8	8.2	988.3	2.0	665.9	26.5	0.04
NW10_06_9	2.893	0.044	0.2153	0.0031	0.99	4.64	0.07	0.0971	0.0002	−0.26	0.066	0.001	1228.3	25.0	1256.3	16.2	1379.0	11.4	1569.5	3.2	559.0	111.1	0.20
NW10_06_10	3.590	0.048	0.2599	0.0034	0.99	3.85	0.05	0.0998	0.0002	0.00	0.078	0.001	1471.7	29.2	1488.7	17.5	1546.5	10.5	1620.9	2.8	575.6	111.1	0.19
NW10_06_11	3.858	0.049	0.2738	0.0035	0.98	3.65	0.05	0.1018	0.0003	0.04	0.077	0.001	1548.1	30.5	1559.3	17.6	1603.1	10.3	1656.6	4.2	609.2	71.2	0.12
NW10_06_12	3.143	0.044	0.2412	0.0033	0.97	4.15	0.06	0.0941	0.0003	0.08	0.074	0.001	1382.6	27.9	1392.3	17.0	1442.7	10.9	1509.3	4.8	149.1	163.6	1.10
NW10_06_13	1.659	0.023	0.1657	0.0023	0.98	6.03	0.08	0.0725	0.0002	0.02	0.051	0.007	987.8	19.9	988.1	12.5	992.8	8.7	999.9	2.3	444.0	5.8	0.01
NW10_06_14	1.622	0.020	0.1619	0.0020	0.98	6.18	0.07	0.0725	0.0002	−0.05	0.054	0.002	965.7	18.6	966.9	10.8	979.5	7.8	1001.0	2.4	563.8	15.3	0.03
NW10_06_15	1.562	0.019	0.1570	0.0020	0.99	6.37	0.08	0.0718	0.0001	0.04	0.042	0.001	939.3	18.3	939.9	10.9	954.2	7.6	980.5	1.6	1155.7	47.2	0.04
NW10_06_16	3.792	0.059	0.2767	0.0041	0.99	3.61	0.05	0.0992	0.0002	−0.09	0.078	0.001	1573.1	33.0	1576.0	20.3	1593.6	12.3	1609.4	2.9	379.7	65.7	0.17
NW10_06_17	1.992	0.028	0.1806	0.0025	0.97	5.54	0.08	0.0799	0.0003	−0.04	0.069	0.001	1065.7	21.5	1070.0	13.7	1112.3	9.5	1193.3	3.8	240.4	42.6	0.18
NW10_06_18	1.591	0.019	0.1594	0.0019	0.99	6.27	0.08	0.0721	0.0001	0.00	0.048	0.001	953.4	18.1	953.0	10.6	965.8	7.4	989.7	1.9	948.6	37.2	0.04
NW10_06_19	1.601	0.022	0.1612	0.0021	0.99	6.20	0.08	0.0720	0.0001	−0.01	0.049	0.001	964.5	18.9	963.0	11.8	971.9	8.7	987.2	2.0	785.0	30.3	0.04
NW10_06_20	2.522	0.033	0.2099	0.0027	0.99	4.76	0.06	0.0868	0.0002	−0.12	0.059	0.001	1224.5	24.0	1227.9	14.2	1277.1	9.5	1355.3	3.0	592.6	37.1	0.06
NW10_06_21	1.579	0.024	0.1461	0.0022	0.94	6.85	0.10	0.0781	0.0004	0.07	0.056	0.001	872.2	18.3	878.5	12.5	962.2	9.8	1148.2	5.8	121.8	31.5	0.26
NW10_06_22	3.683	0.046	0.2628	0.0033	0.99	3.81	0.05	0.1010	0.0002	−0.06	0.084	0.001	1489.6	28.7	1503.3	16.6	1566.9	10.1	1642.8	2.8	698.7	95.6	0.14
NW10-50, layer-parallel leucosome (*UTM*: *383738, 6958619*)																							
NW10_50_3	1.552	0.022	0.1583	0.0022	0.98	6.32	0.09	0.0707	0.0002	0.04	0.048	0.001	947.1	19.0	946.9	12.1	951.3	8.9	948.1	2.9	1083.1	44.2	0.04
NW10_50_4	3.887	0.069	0.2616	0.0040	0.89	3.82	0.06	0.1070	0.0008	0.05	0.091	0.002	1471.3	31.2	1497.4	20.4	1608.5	14.5	1748.9	12.7	104.7	51.2	0.49
NW10_50_5	1.484	0.025	0.1520	0.0026	0.98	6.58	0.11	0.0707	0.0002	0.24	0.069	0.002	910.7	20.4	911.9	14.6	922.7	10.1	949.7	2.8	1154.4	29.2	0.03
NW10_50_6	3.560	0.068	0.2634	0.0045	0.92	3.80	0.07	0.0983	0.0007	−0.02	0.086	0.002	1498.3	33.8	1506.2	23.0	1542.2	14.9	1592.5	12.0	125.2	64.8	0.52
NW10_50_7	1.468	0.022	0.1537	0.0023	0.98	6.50	0.10	0.0697	0.0002	0.05	0.049	0.001	922.0	19.3	921.6	12.9	916.4	9.2	918.7	2.2	1713.2	288.5	0.17
NW10_50_8	1.624	0.031	0.1678	0.0034	0.96	5.96	0.12	0.0713	0.0004	0.16	0.051	0.001	1001.3	24.5	1001.5	18.2	980.8	12.1	967.4	5.3	1115.9	366.4	0.33
NW10_50_9	1.300	0.024	0.1350	0.0019	0.75	7.41	0.11	0.0708	0.0009	0.07	0.040	0.001	811.9	16.6	816.3	11.0	844.4	10.4	952.8	11.5	357.6	372.0	1.04
NW10_50_10	1.426	0.025	0.1533	0.0025	0.95	6.52	0.11	0.0685	0.0003	−0.08	0.045	0.001	920.7	20.1	920.6	14.3	901.3	10.4	884.0	4.2	661.0	24.9	0.04
NW10_50_11	1.729	0.049	0.1722	0.0047	0.97	5.81	0.16	0.0749	0.0005	−0.20	0.065	0.003	1022.4	31.1	1027.9	25.1	1020.8	18.9	1066.2	6.9	373.1	23.7	0.06
NW10_50_14	1.118	0.021	0.1205	0.0019	0.83	8.30	0.13	0.0683	0.0007	0.03	0.036	0.001	729.5	15.7	733.5	11.0	760.7	9.9	876.4	9.3	227.8	235.6	1.03
NW10_50_15	1.113	0.023	0.1209	0.0021	0.92	8.27	0.14	0.0679	0.0005	−0.09	0.036	0.001	732.1	16.5	736.9	12.2	759.1	10.8	865.4	6.1	289.1	388.4	1.34
NW10_50_16	1.588	0.021	0.1647	0.0023	0.98	6.07	0.08	0.0713	0.0002	0.09	0.048	0.002	983.3	19.8	982.3	12.6	964.5	8.4	966.9	2.3	1512.2	49.3	0.03
NW10_50_17	1.550	0.022	0.1610	0.0024	0.98	6.21	0.09	0.0710	0.0002	0.09	0.049	0.001	962.2	20.1	963.3	13.1	951.8	8.9	958.2	2.4	1054.8	45.6	0.04
NW10_50_18	1.530	0.023	0.1593	0.0024	0.99	6.28	0.09	0.0710	0.0002	0.12	0.047	0.001	952.7	19.9	952.6	13.3	941.4	9.1	958.0	2.2	1228.6	46.2	0.04
NW10_50_19	1.588	0.025	0.1640	0.0028	0.96	6.10	0.10	0.0716	0.0003	0.05	0.040	0.001	979.5	21.7	978.8	15.2	964.5	10.0	973.6	4.0	493.8	311.0	0.63
NW10_50_21	1.424	0.024	0.1487	0.0023	0.96	6.73	0.10	0.0708	0.0003	−0.02	0.046	0.001	891.3	18.9	893.3	12.9	898.9	10.2	952.2	4.7	395.6	46.2	0.12
NW10_50_22	2.137	0.043	0.1684	0.0027	0.96	5.94	0.10	0.0942	0.0005	−0.28	0.077	0.002	975.7	21.3	1002.9	15.1	1161.6	13.5	1511.7	7.6	310.8	34.7	0.11
NW10_50_23	1.323	0.022	0.1389	0.0023	0.99	7.20	0.12	0.0700	0.0001	−0.02	0.041	0.001	835.3	18.2	839.5	12.7	854.8	9.6	929.8	1.9	2346.7	56.4	0.02
NW10_50_24	1.453	0.024	0.1499	0.0023	0.99	6.67	0.10	0.0711	0.0001	−0.06	0.045	0.001	898.1	19.1	900.1	13.0	909.8	9.8	959.4	1.9	2409.3	87.8	0.04
NW10_50_25	1.444	0.026	0.1497	0.0027	0.99	6.68	0.12	0.0707	0.0002	−0.17	0.046	0.001	897.3	20.5	898.9	15.0	906.1	10.8	948.8	2.4	1493.1	50.2	0.03
NW10_50_26	1.569	0.027	0.1604	0.0027	0.99	6.24	0.10	0.0717	0.0002	0.02	0.047	0.001	958.0	21.2	961.9	15.0	957.0	10.6	977.2	2.1	2168.7	55.8	0.03
NW10_50_27	3.158	0.053	0.2418	0.0040	0.97	4.14	0.07	0.0961	0.0004	0.04	0.079	0.001	1382.5	30.5	1395.3	20.8	1444.9	12.9	1549.3	5.9	398.1	131.3	0.33
NW10_50_28	4.174	0.080	0.2937	0.0056	0.98	3.40	0.07	0.1037	0.0004	−0.09	0.081	0.002	1656.0	40.0	1658.7	28.0	1672.6	16.1	1692.0	6.7	254.3	152.2	0.60
NW10_50_29	1.687	0.034	0.1706	0.0033	0.99	5.86	0.11	0.0721	0.0001	−0.09	0.047	0.001	1016.4	24.6	1014.6	18.4	1003.0	13.0	990.2	1.9	1876.1	496.9	0.26
NW10_50_30	1.791	0.037	0.1791	0.0035	0.95	5.58	0.11	0.0730	0.0004	−0.24	0.046	0.001	1064.3	25.6	1061.3	19.0	1041.8	13.8	1014.8	5.7	379.7	365.4	0.96
NW10_50_31	1.522	0.022	0.1560	0.0021	0.98	6.41	0.09	0.0712	0.0002	−0.06	0.047	0.001	933.2	18.7	934.1	12.0	938.5	8.8	962.3	2.5	1016.4	39.2	0.04
NW10_50_32	1.339	0.025	0.1289	0.0022	0.89	7.76	0.13	0.0756	0.0006	0.07	0.043	0.001	771.3	17.4	783.0	13.0	864.4	11.1	1085.4	9.2	281.6	307.4	1.09
NW10_50_33	3.605	0.066	0.2630	0.0047	0.97	3.80	0.07	0.1001	0.0004	−0.03	0.075	0.001	1492.6	34.5	1504.0	24.1	1551.8	14.0	1625.4	6.1	263.5	60.5	0.23
NW10_50_34	4.269	0.073	0.2988	0.0055	0.95	3.35	0.06	0.1038	0.0006	0.03	0.083	0.002	1684.3	39.7	1684.0	27.1	1685.2	14.2	1693.3	10.3	96.3	65.9	0.68
NW10_50_35	1.307	0.022	0.1363	0.0022	0.99	7.34	0.12	0.0701	0.0001	0.03	0.044	0.001	819.9	17.7	823.3	12.4	848.6	9.7	930.6	1.6	3358.9	99.8	0.03
NW10_50_36	1.419	0.022	0.1475	0.0022	0.95	6.78	0.10	0.0698	0.0004	0.00	0.044	0.001	885.3	18.3	886.4	12.1	897.2	9.1	923.9	4.8	374.9	215.5	0.57

NW10_50_37	1.596	0.028	0.1616	0.0027	0.98	6.19	0.11	0.0715	0.0002	0.01	0.046	0.001	965.5	21.5	967.2	15.0	968.6	11.1	972.5	2.8	814.8	309.2	0.38
NW10_50_38	1.682	0.024	0.1714	0.0026	0.97	5.83	0.09	0.0714	0.0003	0.15	0.047	0.001	1022.2	21.6	1019.5	14.4	1000.6	9.3	970.2	3.4	882.1	424.8	0.48
NW10_50_39	2.452	0.047	0.1982	0.0038	0.98	5.05	0.10	0.0899	0.0003	0.01	0.067	0.001	1148.8	27.4	1167.1	20.0	1257.5	13.6	1422.8	5.0	411.5	92.7	0.23
NW10_50_40	2.294	0.050	0.1968	0.0037	0.96	5.08	0.10	0.0843	0.0005	−0.29	0.067	0.002	1149.6	27.2	1157.5	20.0	1209.6	15.6	1298.5	7.8	416.9	43.2	0.10
NW10_50_41	1.541	0.019	0.1566	0.0020	0.99	6.38	0.08	0.0715	0.0002	0.03	0.047	0.001	936.7	18.3	937.8	11.2	946.1	7.7	971.1	2.1	2339.5	49.5	0.02
NW10_50_42	1.526	0.024	0.1556	0.0023	0.96	6.43	0.10	0.0713	0.0003	−0.06	0.046	0.001	931.2	19.5	932.2	13.1	939.8	9.7	965.1	3.9	443.0	199.3	0.45
NW10_50_43	1.592	0.018	0.1590	0.0019	0.95	6.29	0.08	0.0724	0.0003	−0.01	0.054	0.001	949.0	18.0	950.8	10.5	966.6	7.1	998.3	3.7	620.8	56.5	0.09
NW10_50_47	1.510	0.026	0.1570	0.0027	0.97	6.37	0.11	0.0697	0.0003	−0.07	0.046	0.001	940.9	20.9	939.7	14.8	933.1	10.7	921.0	3.9	495.7	74.5	0.15
NW10_50_48	4.108	0.065	0.2860	0.0042	0.97	3.50	0.05	0.1032	0.0003	−0.07	0.082	0.001	1614.4	33.8	1623.2	21.4	1654.1	12.8	1682.9	5.5	365.1	113.6	0.31
NW10_50_49	3.603	0.070	0.2596	0.0047	0.98	3.85	0.07	0.1002	0.0004	−0.38	0.080	0.002	1473.6	34.3	1486.9	24.2	1553.3	15.9	1628.5	6.8	495.7	141.4	0.29
NW10_50_50	1.695	0.030	0.1722	0.0031	0.98	5.81	0.11	0.0708	0.0003	0.00	0.047	0.001	1027.8	23.8	1025.8	17.0	1007.7	11.2	952.5	3.6	406.5	461.3	1.13
NW10_50_51	1.562	0.027	0.1581	0.0025	0.93	6.32	0.10	0.0711	0.0005	−0.01	0.047	0.001	945.7	20.2	946.0	13.8	953.9	10.6	961.6	6.3	260.8	405.2	1.55
NW10_50_52	1.414	0.029	0.1465	0.0027	0.98	6.83	0.12	0.0692	0.0002	−0.17	0.044	0.001	880.2	20.4	880.7	15.0	893.0	12.1	905.9	3.1	659.6	39.8	0.06
NW10_50_1_run2	0.807	0.013	0.0917	0.0014	0.98	10.90	0.17	0.0638	0.0002	−0.20	0.036	0.001	562.2	12.1	565.5	8.5	599.9	7.4	734.2	2.4	1045.9	24.2	0.02
NW10_50_2_run2	1.832	0.029	0.1697	0.0026	0.99	5.89	0.09	0.0779	0.0002	−0.20	0.058	0.001	1004.1	21.2	1010.0	14.3	1055.3	10.4	1143.7	2.4	722.9	32.2	0.04
NW10_50_3_run2	3.950	0.057	0.2855	0.0040	0.98	3.50	0.05	0.0997	0.0003	0.02	0.082	0.001	1618.9	33.1	1617.9	20.1	1623.9	11.5	1618.7	4.8	109.1	41.5	0.38
NW10_50_4_run2	1.668	0.027	0.1675	0.0028	0.98	5.97	0.10	0.0717	0.0002	0.17	0.045	0.001	998.9	22.0	998.8	15.2	995.6	10.1	978.7	2.4	859.3	509.2	0.59
NW10_50_5_run2	1.633	0.022	0.1553	0.0020	0.98	6.44	0.08	0.0758	0.0002	−0.16	0.074	0.002	923.8	18.0	930.3	11.1	983.7	8.7	1089.4	3.0	1367.8	44.1	0.03
NW10_50_2_run3_rim	1.360	0.015	0.1398	0.0013	0.94	7.15	0.07	0.0708	0.0003	−0.10	0.043	0.000	839.6	14.7	843.3	7.4	871.7	6.2	950.3	3.9	367.5	403.0	1.10
NW10_50_4_run3_rim	1.245	0.013	0.1337	0.0013	0.93	7.48	0.07	0.0677	0.0003	0.07	0.042	0.000	807.3	14.2	808.9	7.2	821.4	5.6	860.1	3.2	195.8	109.9	0.56
NW10_50_5_run3_rim	1.564	0.016	0.1607	0.0015	0.93	6.22	0.06	0.0707	0.0003	−0.04	0.049	0.000	961.1	16.8	961.3	8.2	955.4	6.4	950.1	3.6	177.6	180.3	1.02
NW10_50_6_run3_rim	3.553	0.043	0.2566	0.0030	0.99	3.90	0.05	0.1013	0.0002	−0.17	0.086	0.001	1455.0	27.6	1472.1	15.5	1538.7	9.4	1648.8	3.8	357.7	372.1	1.04
NW10_50_7_run3_rim	1.408	0.015	0.1427	0.0016	0.99	7.01	0.08	0.0722	0.0001	−0.20	0.047	0.001	855.3	15.7	860.0	8.8	892.9	6.7	991.6	1.9	880.1	31.1	0.04
NW10_50_8_run3_rim	1.163	0.013	0.1261	0.0014	0.96	7.93	0.09	0.0678	0.0002	0.02	0.040	0.001	762.5	14.0	765.3	7.8	783.3	6.0	861.8	3.0	311.5	376.9	1.21
NW10_50_9_run3	4.770	0.047	0.3074	0.0029	0.98	3.25	0.03	0.1138	0.0002	−0.05	0.089	0.001	1708.8	30.3	1727.3	14.3	1779.4	8.3	1861.1	3.2	720.4	94.3	0.13
NW10_50_10_run3	1.672	0.020	0.1620	0.0018	0.96	6.17	0.07	0.0759	0.0002	−0.03	0.058	0.001	962.4	17.8	967.8	10.0	998.6	7.7	1093.2	2.8	471.3	26.0	0.06
NW10_50_11_run3	4.042	0.050	0.2810	0.0031	0.98	3.56	0.04	0.1052	0.0002	−0.30	0.093	0.001	1581.8	29.4	1595.6	15.7	1643.0	10.0	1718.3	3.4	473.3	209.9	0.44
NW10_50_12_run3	1.519	0.026	0.1570	0.0024	0.96	6.37	0.10	0.0707	0.0003	−0.10	0.045	0.000	939.7	19.9	939.6	13.5	939.4	10.2	948.9	4.2	168.7	144.9	0.86
NW10_50_4_run4	1.556	0.020	0.1542	0.0020	0.97	6.48	0.08	0.0735	0.0002	−0.03	0.046	0.001	920.3	17.9	924.2	11.0	951.7	8.2	1026.8	3.1	740.6	34.9	0.05
NW10_50_5_run4	3.900	0.059	0.2668	0.0039	0.98	3.75	0.05	0.1064	0.0003	−0.13	0.084	0.001	1500.8	31.0	1523.3	19.6	1611.1	12.3	1738.4	4.8	308.8	117.8	0.38
NW10_50_6_run4	1.259	0.017	0.1329	0.0018	0.95	7.53	0.10	0.0690	0.0003	0.13	0.040	0.001	801.0	16.0	803.9	10.3	826.3	7.9	899.4	3.9	220.8	188.6	0.85
NW10_50_7_run4	1.341	0.018	0.1399	0.0019	0.97	7.15	0.10	0.0697	0.0003	−0.13	0.042	0.001	841.2	16.7	843.6	10.6	862.6	7.8	920.3	3.3	254.4	283.0	1.11
NW10_50_9_run4	4.087	0.056	0.2831	0.0039	0.98	3.53	0.05	0.1051	0.0003	0.10	0.082	0.001	1594.1	32.2	1606.0	19.5	1649.7	11.1	1715.3	4.5	269.1	157.7	0.59
NW10_50_10_run4	3.814	0.059	0.2690	0.0040	0.98	3.72	0.05	0.1031	0.0003	−0.12	0.078	0.001	1519.7	31.7	1534.4	20.2	1592.9	12.6	1680.6	5.2	150.6	104.0	0.69
NW10_50_1_run5	3.968	0.039	0.2867	0.0030	0.98	3.49	0.04	0.1003	0.0003	0.18	0.083	0.002	1624.4	29.6	1624.3	15.0	1626.7	8.0	1628.8	4.4	239.3	27.0	0.11
NW10_50_2_run5	0.629	0.008	0.0705	0.0009	0.68	14.19	0.18	0.0648	0.0006	0.42	0.057	0.002	433.8	8.4	438.8	6.6	495.4	4.6	768.4	7.1	968.2	59.3	0.06
NW10_50_3_run5	1.330	0.023	0.1384	0.0021	0.98	7.23	0.11	0.0699	0.0003	−0.57	0.041	0.001	832.4	17.5	835.2	11.9	860.7	9.7	925.9	4.4	1014.4	462.8	0.46
NW10_50_4_run5	0.465	0.006	0.0623	0.0008	0.96	16.06	0.20	0.0548	0.0002	−0.03	0.020	0.000	389.2	7.5	389.3	5.8	387.5	4.3	402.2	1.5	821.1	61.9	0.08
NW10_50_5_run5	1.558	0.023	0.1507	0.0019	0.96	6.63	0.08	0.0758	0.0003	−0.22	0.074	0.002	897.5	17.5	904.8	10.8	955.2	9.0	1091.1	4.5	723.1	41.8	0.06
NW10_50_6_run5	1.561	0.022	0.1609	0.0022	0.98	6.22	0.08	0.0714	0.0002	0.02	0.046	0.001	961.3	19.1	962.6	12.3	955.5	8.7	969.6	3.0	385.1	269.8	0.70
NW10_50_7_run5	1.547	0.019	0.1605	0.0018	0.91	6.23	0.07	0.0708	0.0004	−0.02	0.046	0.001	959.6	17.9	959.1	10.2	948.4	7.7	951.7	5.1	99.9	103.4	1.04
NW10_50_2_run3 core	1.478	0.020	0.1517	0.0019	0.89	6.59	0.08	0.0708	0.0004	0.08	0.047	0.001	908.8	17.4	910.1	10.4	920.2	8.3	951.0	5.9	86.1	70.0	0.81
NW10_50_4_run3 core	1.261	0.020	0.1329	0.0020	0.98	7.52	0.11	0.0688	0.0002	−0.22	0.043	0.001	801.7	16.8	804.3	11.3	827.0	9.0	894.1	2.6	487.2	217.6	0.45
NW10_50_5_run3 core	1.124	0.019	0.1150	0.0013	0.63	8.69	0.10	0.0711	0.0008	−0.11	0.037	0.001	694.5	12.9	701.7	7.5	763.4	9.1	961.5	11.4	518.3	510.4	0.98
NW10_50_6_run3 core	0.960	0.013	0.1057	0.0013	0.97	9.46	0.12	0.0660	0.0002	−0.08	0.034	0.000	643.6	12.5	647.3	7.8	682.6	6.6	807.4	2.5	549.1	751.0	1.37
NW10_50_7_run3 core	1.542	0.019	0.1573	0.0018	0.96	6.36	0.07	0.0713	0.0002	0.03	0.046	0.001	940.7	17.6	941.5	10.2	946.3	7.7	967.3	3.2	251.4	381.5	1.52
NW10_50_8_run3 core	4.372	0.055	0.2955	0.0037	0.99	3.38	0.04	0.1075	0.0002	0.04	0.091	0.001	1657.3	32.3	1668.0	18.5	1705.2	10.5	1757.8	3.5	341.6	297.6	0.87
NW10-54, layer-parallel leucosome (*UTM*: *371945, 6965140*)																							
NW10_54_1 rim	0.480	0.007	0.0635	0.0009	0.88	15.76	0.22	0.0553	0.0004	0.06	0.005	0.005	396.4	8.1	396.6	5.4	398.9	4.7	422.8	2.9	168.3	1.1	0.01
NW10_54_2 rim	0.490	0.007	0.0648	0.0008	0.92	15.43	0.19	0.0551	0.0003	0.01	0.006	0.013	404.7	7.8	404.8	4.9	404.4	4.5	417.9	2.3	347.4	2.4	0.01
NW10_54_4 rim	0.544	0.009	0.0693	0.0011	0.93	14.43	0.23	0.0572	0.0004	−0.06	0.019	0.031	431.0	9.3	431.7	6.4	440.3	6.2	500.0	3.2	207.6	1.9	0.01
NW10_54_5 rim	0.483	0.008	0.0639	0.0009	0.94	15.65	0.23	0.0550	0.0003	−0.14	0.019	0.012	399.0	8.3	399.1	5.6	399.9	5.4	411.0	2.4	276.1	2.2	0.01
NW10_54_6 rim	0.499	0.007	0.0655	0.0009	0.93	15.26	0.20	0.0548	0.0003	0.01	0.000	0.012	409.1	8.1	409.0	5.2	410.3	4.9	404.9	2.3	253.5	2.1	0.01
NW10_54_7 rim	0.499	0.014	0.0631	0.0011	0.62	15.85	0.28	0.0569	0.0012	0.05	0.001	0.003	393.3	9.0	394.3	6.7	410.9	9.1	487.7	10.3	26.3	0.2	0.01
NW10_54_8 rim	0.498	0.013	0.0638	0.0010	0.69	15.67	0.25	0.0563	0.0010	−0.09	<	<	397.9	8.6	398.5	6.3	410.9	9.0	464.2	8.2	39.9	0.2	0.01
NW10_54_9 rim	0.485	0.008	0.0639	0.0010	0.96	15.65	0.24	0.0550	0.0002	0.04	0.010	0.010	399.2	8.6	399.1	6.2	401.3	5.5	410.2	1.8	328.1	2.2	0.01

(continued on next page)

Table 1 (*continued*)

Sample, grain number*	$^{207}Pb/^{235}U$	±2σ%	$^{206}Pb/^{238}U$	±2σ%	Error correlation	$^{238}U/^{206}Pb$	±2σ%	$^{207}Pb/^{206}Pb$	±2σ%	Error correlation	$^{208}Pb/^{232}Th$	±2σ%	207-corrected age*	Error	$^{206}Pb/^{238}U$ date (Ma)	±2σ abs	$^{207}Pb/^{235}U$ date (Ma)	±2σ abs	$^{207}Pb/^{206}Pb$ date (Ma)	±2σ abs	Approx. U (ppm)	Approx. Th (ppm)	Th/U
NW10-54, layer-parallel leucosome (*UTM*: *371945, 6965140*)																							
NW10_54_10 rim	0.485	0.007	0.0636	0.0008	0.84	15.72	0.20	0.0551	0.0004	0.12	0.007	0.012	397.3	7.8	397.4	4.9	401.5	4.4	415.9	3.1	184.0	2.0	0.01
NW10_54_11	0.491	0.006	0.0647	0.0008	0.95	15.45	0.19	0.0547	0.0002	0.18	0.024	0.012	404.4	7.8	404.2	4.9	405.4	4.0	401.2	1.7	381.9	3.2	0.01
NW10_54_12	0.528	0.009	0.0669	0.0010	0.95	14.95	0.22	0.0570	0.0003	−0.08	0.048	0.010	416.5	8.7	417.5	6.2	430.0	5.9	491.1	2.8	340.4	4.7	0.01
NW10_54_13	0.493	0.007	0.0652	0.0009	0.94	15.33	0.21	0.0546	0.0003	0.00	0.015	0.013	407.5	8.2	407.3	5.4	406.9	4.6	393.8	2.1	295.6	1.4	0.00
NW10_54_14	0.597	0.011	0.0719	0.0013	0.94	13.91	0.25	0.0605	0.0004	−0.08	0.044	0.035	445.0	10.3	447.2	7.7	475.3	7.2	621.1	4.1	167.6	2.8	0.02
NW10_54_1 core	0.478	0.007	0.0630	0.0007	0.70	15.87	0.18	0.0549	0.0010	0.07	0.002	0.004	393.9	7.3	393.9	4.2	396.2	4.9	406.9	7.4	92.0	0.6	0.01
NW10_54_2 core	0.485	0.006	0.0639	0.0007	0.92	15.65	0.17	0.0551	0.0009	−0.08	0.023	0.013	399.2	7.3	399.3	4.2	401.5	3.8	414.7	6.5	407.4	3.8	0.01
NW10_54_3 core	3.330	0.052	0.2422	0.0034	0.94	4.13	0.06	0.0996	0.0016	−0.07	0.075	0.001	1378.2	28.2	1398.0	18.0	1487.0	12.0	1616.1	25.7	86.1	69.8	0.81
NW10_54_4 core	3.394	0.050	0.2439	0.0033	0.99	4.10	0.06	0.1008	0.0015	−0.38	0.078	0.001	1385.4	27.9	1406.0	17.0	1501.0	12.0	1638.5	24.9	300.2	433.0	1.44
NW10_54_5 core	0.489	0.007	0.0644	0.0008	0.93	15.52	0.19	0.0549	0.0009	−0.15	0.029	0.032	402.4	7.7	402.5	4.6	403.9	4.5	409.8	6.5	319.8	2.7	0.01
NW10_54_6 core	0.503	0.008	0.0653	0.0009	0.82	15.31	0.22	0.0558	0.0010	0.10	<	<	407.3	8.3	407.7	5.6	413.1	5.4	444.0	7.8	192.5	2.4	0.01
NW10_54_7 core	0.492	0.007	0.0643	0.0008	0.92	15.56	0.20	0.0555	0.0009	−0.04	<	<	401.2	7.9	401.5	5.0	406.2	4.8	432.4	6.9	335.9	1.4	0.00
NW10_54_8 core	0.485	0.006	0.0640	0.0007	0.91	15.63	0.18	0.0549	0.0009	0.05	<	<	399.8	7.5	399.8	4.5	401.2	4.1	408.6	6.5	282.8	2.5	0.01
NW10_54_9 core	1.876	0.025	0.1505	0.0018	0.95	6.64	0.08	0.0904	0.0014	−0.03	0.052	0.001	879.4	16.8	903.0	10.0	1071.4	8.6	1434.4	22.3	192.0	42.7	0.22
NW10_54_10 core	2.647	0.033	0.1969	0.0023	0.98	5.08	0.06	0.0976	0.0015	−0.17	0.076	0.002	1130.2	21.4	1158.0	12.0	1313.5	9.5	1577.8	24.1	419.0	28.8	0.07
NW10-56, layer-parallel leucosome (*UTM*: *371945, 6965140*)																							
NW10_56_1 rim	0.498	0.005	0.0655	0.0006	0.77	15.26	0.13	0.0554	0.0009	0.07	0.021	0.020	408.9	7.0	409.2	3.4	410.4	3.6	428.4	7.0	155.9	1.4	0.01
NW10_56_2 rim	2.393	0.027	0.1850	0.0018	0.97	5.41	0.05	0.0945	0.0014	−0.25	0.059	0.001	1068.3	19.1	1094.1	9.8	1241.1	8.1	1517.1	23.2	198.9	41.1	0.21
NW10_56_4 rim	0.494	0.007	0.0656	0.0006	0.53	15.23	0.13	0.0544	0.0010	0.09	<	<	410.1	7.1	409.8	3.5	407.5	4.9	387.6	7.4	68.3	0.8	0.01
NW10_56_5 rim	0.512	0.007	0.0673	0.0007	0.74	14.87	0.15	0.0554	0.0010	0.05	0.009	0.011	419.5	7.6	419.6	4.2	419.3	4.7	427.2	7.5	128.1	0.8	0.01
NW10_56_6 rim	0.490	0.004	0.0651	0.0005	0.81	15.36	0.13	0.0547	0.0009	0.14	0.010	0.007	406.6	6.9	406.6	3.2	404.8	3.0	400.4	6.4	236.7	1.8	0.01
NW10_56_8	2.325	0.045	0.1827	0.0027	0.94	5.47	0.08	0.0923	0.0015	−0.32	0.071	0.002	1058.4	22.1	1081.0	15.0	1218.0	14.0	1473.8	24.1	67.5	18.9	0.28
NW10_56_10	0.501	0.005	0.0655	0.0006	0.87	15.26	0.15	0.0553	0.0009	−0.04	0.005	0.023	409.0	7.3	409.5	3.8	412.6	3.7	422.8	6.8	219.7	1.0	0.00
NW10_56_11	0.494	0.005	0.0649	0.0005	0.80	15.41	0.13	0.0549	0.0009	0.00	0.003	0.007	405.3	6.9	405.2	3.3	407.4	3.4	406.9	6.6	220.4	1.6	0.01
NW10_56_12	0.491	0.005	0.0644	0.0005	0.78	15.53	0.13	0.0550	0.0009	0.05	0.007	0.007	402.1	6.9	402.2	3.2	405.2	3.2	411.0	6.7	203.2	1.9	0.01
NW10_56_13	3.576	0.043	0.2554	0.0029	0.98	3.92	0.04	0.1013	0.0015	−0.24	0.080	0.001	1448.1	27.2	1466.0	15.0	1544.6	9.5	1648.1	25.0	260.7	45.9	0.18
NW10_56_14	0.488	0.006	0.0642	0.0007	0.77	15.59	0.16	0.0551	0.0009	0.08	0.004	0.005	400.7	7.3	400.9	4.1	403.7	4.1	416.7	7.0	169.2	1.1	0.01
NW10_56_15	0.499	0.005	0.0654	0.0006	0.92	15.30	0.15	0.0551	0.0009	0.14	0.021	0.004	408.0	7.2	408.1	3.8	410.5	3.4	417.9	6.5	641.4	5.6	0.01
NW10_56_16	0.495	0.005	0.0651	0.0006	0.88	15.37	0.13	0.0549	0.0009	−0.03	0.012	0.008	406.4	7.0	406.4	3.5	408.4	3.5	408.6	6.4	343.0	2.1	0.01
NW10_56_17	0.497	0.005	0.0651	0.0006	0.86	15.37	0.14	0.0552	0.0009	0.07	0.005	0.005	406.2	7.1	406.3	3.5	409.1	3.6	418.7	6.7	276.0	1.8	0.01
NW10_56_18	0.487	0.007	0.0637	0.0007	0.67	15.69	0.16	0.0553	0.0010	0.10	<	<	397.9	7.2	398.2	4.0	403.6	4.5	423.2	7.6	81.0	0.8	0.01
NW10_56_19	0.535	0.013	0.0669	0.0010	0.93	14.94	0.22	0.0580	0.0011	−0.65	0.010	0.016	416.1	8.6	418.1	6.0	435.9	8.5	530.9	10.1	146.3	1.7	0.01
NW10_56_20	0.492	0.006	0.0645	0.0006	0.88	15.51	0.15	0.0550	0.0009	0.00	0.015	0.018	402.8	7.2	402.8	3.9	405.8	4.0	411.0	6.7	279.6	1.6	0.01
NW10_56_1 core	2.514	0.024	0.1892	0.0013	0.76	5.29	0.04	0.0965	0.0016	−0.11	0.058	0.001	1088.9	18.1	1117.1	6.9	1275.7	7.0	1557.3	25.3	219.4	44.6	0.20
NW10_56_2 core	0.489	0.004	0.0647	0.0003	0.59	15.45	0.07	0.0548	0.0009	0.07	0.013	0.014	404.3	6.4	404.3	1.8	403.9	2.4	403.3	6.5	267.8	1.8	0.01
NW10_56_3 core	0.488	0.003	0.0642	0.0003	0.61	15.59	0.06	0.0552	0.0009	−0.02	0.013	0.010	400.6	6.2	400.8	1.6	403.6	2.2	418.7	6.7	343.5	2.2	0.01
NW10_56_4 core	0.565	0.020	0.0690	0.0014	0.93	14.49	0.29	0.0592	0.0013	−0.67	0.043	0.024	428.1	10.7	430.1	8.5	454.0	13.0	574.5	12.9	153.8	3.8	0.02
NW10_56_6 core	2.478	0.029	0.1888	0.0017	0.78	5.30	0.05	0.0953	0.0016	−0.08	0.078	0.002	1088.4	19.1	1114.5	9.0	1264.6	8.5	1533.8	25.9	33.5	26.1	0.78
NW10_56_7 core	0.484	0.004	0.0642	0.0004	0.54	15.59	0.09	0.0547	0.0009	0.13	0.007	0.009	400.8	6.4	400.8	2.2	400.7	2.9	398.3	6.6	200.0	1.5	0.01
NW10-12, eclogite-margin leucosome (*UTM*: *307719, 6870092*)																							
NW10_12_2	2.624	0.033	0.2122	0.0023	0.95	4.71	0.05	0.0893	0.0004	−0.24	0.054	0.001	1228.3	22.5	1240.0	12.2	1306.0	9.2	1411.3	5.7	706.5	250.9	0.36
NW10_12_3	1.975	0.025	0.1792	0.0021	0.96	5.58	0.07	0.0797	0.0003	0.05	0.049	0.001	1056.0	20.0	1062.3	11.8	1105.8	8.4	1188.6	4.2	666.5	385.9	0.58
NW10_12_5	1.720	0.046	0.1627	0.0026	0.93	6.15	0.10	0.0762	0.0010	−0.64	0.025	0.000	965.9	20.7	971.2	14.1	1013.3	17.0	1100.6	14.7	372.7	170.7	0.46
NW10_12_8	3.036	0.047	0.2308	0.0034	0.98	4.33	0.06	0.0952	0.0003	−0.05	0.063	0.001	1322.8	27.4	1338.0	17.7	1414.4	11.7	1532.2	4.9	448.2	55.9	0.12
NW10_12_10	2.412	0.029	0.2051	0.0022	0.95	4.87	0.05	0.0853	0.0003	−0.12	0.055	0.001	1195.0	21.9	1202.5	11.9	1246.3	8.9	1322.4	5.2	468.8	103.4	0.22
NW10_12_11	2.178	0.029	0.1893	0.0025	0.96	5.28	0.07	0.0836	0.0003	0.00	0.053	0.001	1107.8	21.8	1117.1	13.4	1172.7	9.2	1284.0	4.6	1166.8	851.0	0.73
NW10_12_13	3.567	0.050	0.2606	0.0034	0.97	3.84	0.05	0.0993	0.0003	−0.18	0.070	0.001	1480.7	29.2	1491.9	17.5	1540.1	11.2	1611.0	5.0	387.1	304.8	0.79
NW10_12_14	3.337	0.054	0.2443	0.0033	0.94	4.09	0.06	0.0994	0.0006	−0.37	0.059	0.001	1390.4	27.9	1408.4	17.1	1488.8	13.0	1612.8	10.2	735.2	87.1	0.12
NW10_12_16	4.105	0.051	0.2857	0.0035	0.95	3.50	0.04	0.1044	0.0004	0.10	0.070	0.001	1610.1	31.1	1619.4	17.6	1654.9	10.5	1704.2	6.5	460.4	75.2	0.16
NW10_12_19	3.315	0.048	0.2507	0.0035	0.98	3.99	0.06	0.0961	0.0003	−0.03	0.074	0.001	1432.1	28.9	1441.4	17.8	1482.6	11.0	1550.1	5.0	162.9	69.6	0.43

NW10-36D, eclogite margin leucosome (*UTM*: *325810, 6920646*)																						
NW10_36D_2 rim	0.478	0.006	0.0637	0.0007	0.71	15.69	0.17	0.0539	0.0009	0.08	0.000	0.001	398.6	7.4	398.2	4.3	396.4	4.1	368.5	6.3	101.2	0.0	0.00
NW10_36D_3 rim	0.482	0.005	0.0634	0.0007	0.95	15.78	0.18	0.0550	0.0008	0.07	0.025	0.007	396.0	7.4	396.1	4.3	399.4	3.7	410.2	6.3	747.0	4.7	0.01
NW10_36D_4 rim	0.492	0.008	0.0646	0.0008	0.71	15.49	0.19	0.0549	0.0010	0.12	0.000	0.001	403.3	7.8	403.3	4.8	406.5	5.4	409.0	7.6	67.9	0.2	0.00
NW10_36D_5 rim	0.482	0.008	0.0634	0.0009	0.76	15.78	0.21	0.0551	0.0010	0.07	0.001	0.001	396.0	7.9	396.2	5.2	400.1	5.3	415.1	7.4	85.6	−0.3	0.00
NW10_36D_6 rim	0.474	0.007	0.0630	0.0007	0.82	15.87	0.17	0.0548	0.0009	−0.03	<	<	393.8	7.2	393.9	4.0	393.9	4.5	402.4	6.7	141.6	0.4	0.00
NW10_36D_7	0.584	0.015	0.0711	0.0011	0.93	14.06	0.22	0.0596	0.0012	−0.61	0.036	0.005	440.6	9.4	442.8	6.8	465.8	9.4	588.0	11.4	262.2	5.7	0.02
NW10_36D_8	3.269	0.034	0.2407	0.0024	0.98	4.15	0.04	0.0989	0.0015	−0.03	0.075	0.001	1371.1	24.7	1390.0	13.0	1473.7	8.0	1603.5	24.3	358.2	204.5	0.57
NW10_36D_9	0.468	0.006	0.0623	0.0008	0.96	16.05	0.20	0.0548	0.0008	−0.07	0.027	0.012	389.4	7.5	389.6	4.6	389.7	4.1	402.0	6.2	554.6	2.8	0.00
NW10_36D_10	0.479	0.006	0.0635	0.0008	0.96	15.76	0.20	0.0546	0.0008	−0.11	0.016	0.008	396.6	7.8	396.5	4.9	397.5	4.4	394.6	6.1	687.0	3.2	0.00
NW10_36D_11	0.489	0.006	0.0642	0.0007	0.97	15.57	0.17	0.0552	0.0008	0.03	0.027	0.001	401.1	7.4	401.3	4.3	404.2	3.7	419.5	6.4	1161.0	12.2	0.01
NW10_36D_12	0.494	0.007	0.0655	0.0009	0.94	15.27	0.20	0.0546	0.0009	−0.02	0.011	0.005	409.0	8.1	409.2	5.2	407.3	4.7	396.7	6.2	409.0	2.5	0.01
NW10_36D_13	0.484	0.005	0.0637	0.0007	0.97	15.69	0.17	0.0549	0.0008	0.05	0.022	0.001	398.2	7.3	398.2	4.2	400.8	3.5	406.1	6.2	1137.0	10.7	0.01
NW10_36D_14	0.481	0.006	0.0632	0.0008	0.98	15.82	0.19	0.0549	0.0008	0.07	0.020	0.001	395.1	7.5	395.2	4.5	398.5	3.9	407.7	6.2	1203.0	10.9	0.01
NW10_36D_15	1.102	0.013	0.1038	0.0011	0.95	9.63	0.10	0.0768	0.0012	−0.16	0.100	0.007	623.9	11.4	636.9	6.3	754.3	6.1	1116.3	17.1	454.9	10.7	0.02
NW10_36D_16	0.488	0.005	0.0645	0.0006	0.89	15.51	0.15	0.0547	0.0009	0.02	<	<	402.7	7.2	403.0	3.8	403.6	3.5	398.3	6.3	326.8	0.0	0.00
NW10_36D_17	0.539	0.022	0.0690	0.0017	0.74	14.49	0.36	0.0565	0.0016	−0.19	0.019	0.017	429.6	12.2	430.0	10.0	440.0	14.0	472.1	13.7	98.0	1.3	0.01
NW10_36D_18	0.497	0.008	0.0650	0.0008	0.81	15.40	0.19	0.0549	0.0010	−0.04	0.003	0.009	405.6	7.8	405.6	4.9	410.2	5.4	408.2	7.1	99.6	0.2	0.00
NW10_36D_19	0.480	0.006	0.0635	0.0007	0.86	15.75	0.18	0.0548	0.0009	0.00	0.001	0.001	396.8	7.4	396.8	4.4	398.1	4.3	404.1	6.6	210.4	−0.2	0.00
NW10_36D_20	0.493	0.006	0.0630	0.0007	0.99	15.87	0.18	0.0564	0.0009	−0.02	0.020	0.000	393.0	7.4	393.9	4.4	406.8	3.9	469.7	7.1	3639.0	51.8	0.01
NW10_36D_21	0.491	0.006	0.0647	0.0008	0.97	15.47	0.20	0.0551	0.0008	0.10	0.021	0.001	403.7	7.9	403.8	4.9	405.4	4.3	414.3	6.3	1060.0	12.3	0.01
NW10_36D_1 core	0.514	0.004	0.0673	0.0004	0.59	14.85	0.08	0.0554	0.0009	0.14	0.036	0.022	419.9	6.7	420.0	2.2	421.2	2.6	426.4	6.9	312.0	4.2	0.01
NW10_36D_2 core	0.483	0.003	0.0635	0.0003	0.73	15.76	0.07	0.0552	0.0009	0.08	0.024	0.003	396.4	6.2	396.7	1.7	400.1	1.8	421.9	6.5	783.0	6.6	0.01
NW10_36D_3 core	0.518	0.005	0.0683	0.0005	0.76	14.64	0.10	0.0549	0.0009	0.04	0.018	0.013	426.2	7.1	426.0	3.0	423.3	3.2	409.8	6.6	316.0	2.0	0.01
NW10_36D_4 core	0.473	0.006	0.0620	0.0003	0.44	16.13	0.08	0.0553	0.0010	−0.06	<	<	387.2	6.2	387.7	1.9	393.8	4.0	424.4	7.9	94.1	−0.1	0.00
NW10_36D_5 core	0.472	0.004	0.0621	0.0003	0.50	16.11	0.07	0.0551	0.0009	−0.03	<	0.003	387.9	6.1	388.2	1.6	392.2	3.0	416.7	7.1	173.4	0.0	0.00
NW10_36D_6 core	0.475	0.004	0.0631	0.0003	0.47	15.85	0.07	0.0547	0.0009	0.12	<	<	394.3	6.2	394.3	1.7	394.8	2.6	400.0	6.6	186.2	0.5	0.00
NW10-36E, eclogite-margin leucosome (*UTM*: *325810, 6920646*)																						
NW10_36E_1	0.996	0.058	0.0984	0.0039	0.99	10.16	0.40	0.0712	0.0015	−0.91	0.061	0.003	596.5	24.8	603.7	22.8	687.1	29.3	963.2	19.9	434.1	21.2	0.05
NW10_36E_2	2.610	0.040	0.1922	0.0030	0.98	5.20	0.08	0.0986	0.0003	0.00	0.093	0.004	1102.6	23.4	1132.7	16.0	1302.6	11.7	1597.9	4.7	883.6	13.3	0.02
NW10_36E_3	4.017	0.064	0.2601	0.0041	0.98	3.84	0.06	0.1118	0.0003	0.00	0.088	0.001	1453.4	31.2	1489.2	20.8	1636.7	13.4	1829.6	5.2	428.0	282.8	0.66
NW10_36E_4	1.593	0.023	0.1584	0.0022	0.98	6.31	0.09	0.0729	0.0002	−0.15	0.045	0.001	945.3	19.2	947.5	12.4	966.2	9.1	1009.9	2.7	708.7	188.0	0.27
NW10_36E_5	2.864	0.060	0.2058	0.0030	0.93	4.86	0.07	0.1005	0.0009	−0.49	0.077	0.002	1175.2	24.4	1205.8	16.0	1368.5	15.6	1633.1	15.4	1000.9	29.0	0.03
NW10_36E_6	0.486	0.008	0.0636	0.0009	0.83	15.71	0.23	0.0553	0.0005	0.09	−0.017	0.030	397.4	8.2	397.7	5.6	402.0	5.5	425.9	4.0	108.3	1.2	0.01
NW10_36E_7	3.193	0.054	0.2161	0.0034	0.99	4.63	0.07	0.1067	0.0003	−0.31	0.098	0.003	1222.2	26.2	1260.7	17.9	1452.5	13.2	1744.6	4.9	400.3	19.5	0.05
NW10_36E_8	9.355	0.182	0.3819	0.0068	0.99	2.62	0.05	0.1767	0.0005	−0.35	0.114	0.002	1939.1	47.4	2086.7	32.6	2370.5	17.6	2621.9	7.5	123.9	70.5	0.57
NW10_36E_9	3.685	0.060	0.2477	0.0040	0.97	4.04	0.07	0.1078	0.0004	−0.01	0.078	0.001	1393.3	30.4	1428.1	20.0	1568.8	12.9	1761.8	6.6	817.3	75.1	0.09
NW10_36E_10	4.346	0.067	0.2805	0.0041	0.98	3.57	0.05	0.1120	0.0003	−0.04	0.085	0.001	1564.6	32.6	1592.5	20.7	1699.5	12.6	1831.4	5.7	545.1	194.0	0.36
NW10_36E_11	1.350	0.022	0.1389	0.0021	0.99	7.20	0.11	0.0703	0.0002	−0.33	0.042	0.001	835.2	17.7	838.3	12.1	865.9	9.3	936.4	2.3	947.8	78.5	0.08
NW10_36E_13	4.078	0.069	0.2809	0.0043	0.98	3.56	0.05	0.1049	0.0004	−0.22	0.086	0.001	1582.0	33.8	1597.2	22.3	1646.7	13.8	1711.9	6.6	181.7	94.5	0.52
NW10_36E_14	3.034	0.042	0.2179	0.0030	0.99	4.59	0.06	0.1011	0.0002	−0.12	0.084	0.001	1241.1	24.9	1270.1	15.7	1415.7	10.8	1644.0	3.9	530.0	179.3	0.34
NW10_36E_16	0.683	0.029	0.0750	0.0020	0.98	13.33	0.35	0.0653	0.0011	−0.81	0.061	0.004	461.0	13.8	465.9	11.9	523.6	16.7	783.5	13.2	933.1	38.0	0.04
NW10_36E_2_run2	1.396	0.016	0.1415	0.0015	0.98	7.07	0.08	0.0717	0.0002	−0.12	0.053	0.001	848.4	15.5	852.7	8.5	886.4	6.6	976.3	2.1	1044.6	72.5	0.07
NW10_36E_4_run2	0.974	0.048	0.0982	0.0030	0.95	10.19	0.31	0.0714	0.0015	−0.65	0.043	0.031	595.1	19.7	605.5	18.0	685.4	24.5	967.6	20.7	367.2	14.4	0.04
NW10_36E_5_run2	4.009	0.048	0.2781	0.0032	0.99	3.60	0.04	0.1049	0.0002	−0.07	0.085	0.001	1566.5	29.5	1583.1	15.8	1634.4	9.8	1712.5	3.3	355.6	222.6	0.63
NW10_36E_6_run2	3.172	0.087	0.2308	0.0051	0.99	4.33	0.10	0.0996	0.0007	−0.79	0.082	0.001	1314.8	34.6	1336.5	26.9	1442.1	22.1	1616.6	10.7	361.6	132.1	0.37
NW10_36E_7_run2	3.575	0.053	0.2541	0.0035	0.99	3.94	0.05	0.1024	0.0003	−0.43	0.080	0.001	1438.5	28.9	1460.9	18.3	1543.2	12.1	1668.5	4.3	678.3	239.9	0.35
NW10_36E_8_run2	3.227	0.055	0.2389	0.0037	0.98	4.19	0.06	0.0985	0.0004	−0.39	0.071	0.001	1361.7	28.9	1380.4	19.1	1462.6	13.2	1595.9	5.8	669.3	159.9	0.24
NW10_36E_9_run2	4.529	0.058	0.3011	0.0037	0.98	3.32	0.04	0.1096	0.0003	−0.08	0.083	0.001	1683.6	32.6	1698.1	18.8	1735.8	10.9	1792.7	5.1	499.1	232.6	0.47
NW10_36E_10_run2	1.213	0.019	0.1220	0.0016	0.92	8.20	0.11	0.0723	0.0004	−0.18	0.039	0.001	734.1	14.6	741.7	9.3	806.5	8.7	995.1	6.2	694.7	528.0	0.76
NW10-45E, eclogite margin leucosome (*UTM*: *383738, 6958619*)																						
NW10_45E_1	2.178	0.036	0.1692	0.0023	0.97	5.91	0.08	0.0932	0.0015	−0.42	0.087	0.002	981.4	19.8	1007.0	13.0	1175.0	11.0	1492.6	23.5	168.0	30.9	0.18
NW10_45E_2	1.112	0.044	0.1112	0.0049	1.00	8.99	0.40	0.0723	0.0012	0.87	0.019	0.000	671.0	30.5	677.0	29.0	758.0	22.0	995.2	16.2	470.0	49.1	0.10
NW10_45E_3	1.384	0.017	0.1428	0.0017	0.97	7.00	0.08	0.0700	0.0011	0.06	0.050	0.001	858.0	16.3	860.5	9.6	881.8	7.3	927.2	14.2	368.0	281.6	0.77
NW10_45E_4	0.858	0.011	0.0977	0.0012	0.93	10.24	0.13	0.0638	0.0010	0.05	0.036	0.000	598.0	11.5	600.6	6.9	629.4	5.9	734.0	11.5	242.9	185.8	0.76

(continued on next page)

Table 1 (*continued*)

Sample, grain number*	$^{207}Pb/^{235}U$	±2σ%	$^{206}Pb/^{238}U$	±2σ%	Error correlation	$^{238}U/^{206}Pb$	±2σ%	$^{207}Pb/^{206}Pb$	±2σ%	Error correlation	$^{208}Pb/^{232}Th$	±2σ%	207-corrected age*	Error	$^{206}Pb/^{238}U$ date (Ma)	±2σ abs	$^{207}Pb/^{235}U$ date (Ma)	±2σ abs	$^{207}Pb/^{206}Pb$ date (Ma)	±2σ abs	Approx. U (ppm)	Approx. Th (ppm)	Th/U
NW10-45E, eclogite margin leucosome (*UTM: 383738, 6958619*)																							
NW10_45E_5	0.480	0.005	0.0631	0.0005	0.85	15.84	0.13	0.0553	0.0009	−0.04	0.018	0.016	394.3	6.7	394.6	3.1	397.9	3.3	423.2	6.8	262.3	2.4	0.01
NW10_45E_6	0.495	0.007	0.0643	0.0007	0.85	15.56	0.17	0.0559	0.0009	−0.09	0.001	0.003	401.0	7.4	401.5	4.2	407.7	4.6	448.0	7.4	148.3	−0.1	0.00
NW10_45E_8	0.482	0.005	0.0644	0.0006	0.92	15.54	0.15	0.0549	0.0009	−0.02	0.025	0.005	402.1	7.2	402.1	3.9	399.8	3.7	409.0	6.4	419.7	4.1	0.01
NW10_45E_9	0.487	0.006	0.0636	0.0008	0.90	15.73	0.19	0.0556	0.0009	0.14	0.013	0.007	396.8	7.5	397.2	4.6	402.6	4.3	435.2	7.0	292.3	2.2	0.01
NW10_45E_10	1.362	0.016	0.1404	0.0016	0.99	7.12	0.08	0.0707	0.0011	−0.10	0.044	0.001	843.3	15.8	846.5	9.0	873.9	6.8	947.6	14.3	880.7	32.9	0.04
NW10_45E_1_run2	0.487	0.008	0.0630	0.0008	0.86	15.87	0.21	0.0546	0.0005	0.08	0.029	0.015	394.0	7.9	394.0	5.1	402.3	5.1	396.9	3.4	442.6	5.0	0.01
NW10_45E_2_run2	0.487	0.007	0.0626	0.0008	0.82	15.97	0.19	0.0551	0.0005	0.23	0.023	0.017	391.2	7.5	391.5	4.6	403.2	4.4	418.1	3.4	380.3	4.2	0.01
NW10_45E_4_run2	0.503	0.009	0.0647	0.0009	0.80	15.46	0.21	0.0556	0.0006	0.01	0.011	0.012	403.7	8.1	404.0	5.4	413.5	6.3	434.9	4.4	244.3	2.3	0.01
NW10_45E_5_run2	0.496	0.010	0.0626	0.0010	0.86	15.97	0.25	0.0567	0.0006	−0.02	0.009	0.008	390.5	8.4	391.6	5.9	408.5	6.7	479.7	4.9	239.3	1.4	0.01
NW10-53B, inter-boudin leucosome (*UTM: 371945, 6965140*)																							
NW10_53b_1	0.496	0.016	0.0640	0.0011	0.40	15.63	0.36	0.0565	0.0018	0.16	<	<	399.0	9.1	399.8	6.4	408.0	11.0	472.1	15.1	15.0	0.1	0.01
NW10_53b_2	0.479	0.012	0.0624	0.0010	0.60	16.03	0.35	0.0556	0.0014	0.09	0.000	0.003	389.6	8.5	389.9	6.1	397.4	8.4	436.4	10.8	33.5	0.4	0.01
NW10_53b_3	0.475	0.010	0.0635	0.0009	0.52	15.76	0.33	0.0541	0.0013	0.21	0.000	0.002	396.8	8.2	396.5	5.5	394.8	6.7	376.5	8.9	34.6	0.2	0.01
NW10_53b_4	0.476	0.009	0.0637	0.0010	0.75	15.71	0.33	0.0538	0.0010	0.07	0.002	0.004	398.3	8.4	397.8	5.8	395.0	6.1	361.8	7.0	75.2	1.3	0.02
NW10_53b_5	0.486	0.012	0.0633	0.0009	0.68	15.79	0.32	0.0559	0.0015	−0.20	0.001	0.002	395.2	8.0	395.8	5.3	404.2	8.7	448.4	11.7	22.0	0.6	0.03
NW10_53b_6	0.475	0.010	0.0628	0.0008	0.64	15.91	0.31	0.0547	0.0012	0.01	0.000	0.004	392.8	7.7	392.8	4.9	395.3	6.5	400.8	8.6	54.2	0.8	0.01
NW10_53b_7	0.474	0.009	0.0632	0.0008	0.68	15.82	0.31	0.0541	0.0011	0.00	0.008	0.010	395.4	7.8	395.6	4.9	393.2	6.4	376.0	7.8	47.6	0.7	0.02
NW10_53b_8	0.488	0.013	0.0630	0.0010	0.58	15.87	0.35	0.0558	0.0015	−0.01	0.001	0.001	393.2	8.5	393.7	6.2	404.6	9.1	444.4	12.3	18.2	0.7	0.04
NW10_53b_9	0.481	0.012	0.0637	0.0009	0.59	15.69	0.32	0.0551	0.0014	0.01	0.000	0.005	398.0	8.2	398.8	5.5	399.3	8.6	416.3	10.4	21.6	0.6	0.03
NW10_53b_10	0.471	0.009	0.0631	0.0009	0.75	15.84	0.32	0.0538	0.0011	−0.01	<	<	395.1	8.0	394.6	5.3	391.2	6.2	364.4	7.3	55.2	0.5	0.01
NW10_53b_11	0.491	0.014	0.0640	0.0009	0.60	15.63	0.33	0.0553	0.0016	−0.10	0.001	0.002	399.6	8.3	399.8	5.6	405.0	10.0	424.4	12.5	19.8	0.1	0.00
NW10_53b_12	0.497	0.013	0.0631	0.0011	0.59	15.85	0.36	0.0564	0.0015	−0.01	0.000	0.002	393.5	9.0	395.2	6.3	409.1	9.1	468.1	12.2	22.7	0.1	0.00
NW10_53b_13	0.477	0.009	0.0627	0.0009	0.79	15.96	0.32	0.0553	0.0011	−0.06	<	<	391.4	7.9	391.7	5.2	396.1	6.0	426.0	8.3	62.0	0.2	0.00
NW10_53b_14	0.481	0.011	0.0631	0.0010	0.58	15.85	0.35	0.0555	0.0013	0.07	0.000	0.002	394.0	8.5	394.4	6.1	399.6	7.6	432.4	10.1	28.1	0.5	0.02
NW10_53b_15	0.486	0.011	0.0628	0.0009	0.49	15.92	0.33	0.0562	0.0014	0.17	<	<	391.8	8.0	392.6	5.3	401.6	7.5	460.3	11.4	24.9	1.1	0.04
NW10_53B_1_run2	0.475	0.009	0.0632	0.0009	0.69	15.83	0.33	0.0547	0.0011	0.07	<	<	394.9	8.2	394.8	5.6	393.9	6.3	400.4	8.2	55.2	0.5	0.01
NW10_53B_2_run2	0.465	0.007	0.0619	0.0009	0.91	16.15	0.34	0.0546	0.0009	0.06	0.033	0.016	387.3	8.1	387.3	5.6	387.0	5.0	395.9	6.5	244.0	3.3	0.01
NW10_53B_3_run2	3.212	0.044	0.2331	0.0030	0.97	4.29	0.08	0.1001	0.0015	−0.07	0.073	0.001	1326.9	26.1	1350.0	16.0	1458.0	11.0	1625.8	24.9	176.2	143.2	0.81
NW10_53B_4_run2	0.462	0.017	0.0618	0.0012	0.58	16.18	0.40	0.0547	0.0019	0.00	<	<	386.4	9.4	386.5	7.3	385.0	12.0	400.0	13.8	13.4	0.4	0.03
NW10_53B_5_run2	0.469	0.015	0.0612	0.0011	0.46	16.34	0.38	0.0559	0.0018	0.17	0.002	0.004	382.1	8.9	382.8	6.4	389.0	10.0	448.4	14.5	15.7	0.2	0.01
NW10_53B_6_run2	0.687	0.011	0.0766	0.0011	0.97	13.05	0.27	0.0652	0.0010	−0.18	0.071	0.003	470.7	9.7	475.7	6.7	530.1	6.6	779.5	12.2	547.0	13.3	0.02
NW10_53B_7_run2	3.394	0.055	0.2436	0.0039	0.99	4.11	0.09	0.1011	0.0015	−0.06	0.078	0.001	1383.1	30.1	1404.0	20.0	1500.0	13.0	1644.8	25.1	214.7	121.0	0.56
NW10_53B_8_run2	0.466	0.009	0.0623	0.0008	0.69	16.05	0.31	0.0542	0.0011	0.04	0.002	0.006	389.7	7.6	389.5	4.8	387.8	5.9	380.6	7.4	81.8	0.7	0.01

NW10-53B, inter-boudin leucosome (*UTM: 371945, 6965140*)																							
NW10_53B_9_run2	0.474	0.010	0.0628	0.0009	0.64	15.93	0.33	0.0548	0.0012	0.01	0.001	0.002	392.2	8.0	392.3	5.3	392.8	6.9	405.3	9.2	42.9	0.5	0.01
NW10_53B_13_run2	0.493	0.010	0.0635	0.0011	0.90	15.75	0.36	0.0561	0.0010	−0.18	0.032	0.022	396.1	9.0	396.5	6.4	405.9	6.7	456.7	8.0	141.4	1.8	0.01
NW10_53B_14_run2	2.991	0.052	0.2154	0.0037	0.98	4.64	0.11	0.1004	0.0015	0.09	0.059	0.001	1228.3	27.7	1257.0	19.0	1402.0	13.0	1632.1	25.0	606.0	186.1	0.31
NW10_53B_15_run2	0.475	0.011	0.0629	0.0010	0.64	15.90	0.34	0.0546	0.0013	−0.01	<	<	393.2	8.3	393.2	5.7	393.4	7.6	397.1	9.3	38.5	0.2	0.00
NW10_53B_16_run2	0.486	0.007	0.0642	0.0009	0.88	15.58	0.31	0.0549	0.0009	0.06	0.011	0.016	401.0	8.0	401.0	5.2	402.3	4.8	408.6	6.7	229.0	2.7	0.01
NW10_53B_17_run2	1.471	0.056	0.1232	0.0035	0.98	8.12	0.26	0.0858	0.0017	−0.84	0.064	0.001	728.5	23.0	748.0	20.0	909.0	24.0	1333.7	26.3	687.0	3.0	0.00
NW10_53B_18_run2	0.463	0.013	0.0621	0.0011	0.67	16.10	0.37	0.0541	0.0014	−0.36	0.001	0.007	388.5	8.9	388.4	6.8	385.2	9.0	375.2	9.5	29.0	172.0	5.94
NW10_53B_19_run2	0.483	0.009	0.0642	0.0010	0.91	15.58	0.34	0.0546	0.0009	0.05	0.010	0.012	401.2	8.6	401.2	6.3	399.3	5.9	395.9	6.7	229.0	0.2	0.00
NW10_53B_20_run2	0.470	0.012	0.0622	0.0010	0.61	16.08	0.35	0.0550	0.0014	0.04	0.001	0.006	388.7	8.5	389.2	6.3	389.7	8.3	412.2	10.3	31.3	3.1	0.10
NW10_53B_21_run2	0.452	0.015	0.0615	0.0011	0.47	16.26	0.38	0.0537	0.0018	0.10	<	<	385.0	8.9	384.5	6.6	377.0	10.0	358.5	12.0	21.4	0.2	0.01
NW10_53B_22_run2	0.484	0.016	0.0624	0.0011	0.54	16.03	0.37	0.0562	0.0018	0.04	0.003	0.002	389.3	9.0	390.3	6.9	399.0	11.0	460.3	14.8	15.3	0.0	0.00
NW10-55, pegmatite (*UTM: 371945, 6965140*)																							
NW10_55_1 rim	0.484	0.008	0.0631	0.0007	0.68	15.84	0.18	0.0553	0.0006	0.04	0.006	0.017	394.3	7.4	394.7	4.3	400.2	5.3	423.2	4.7	74.4	0.5	0.01
NW10_55_2 rim	0.477	0.007	0.0627	0.0008	0.75	15.96	0.19	0.0547	0.0005	0.05	0.023	0.007	391.7	7.5	391.8	4.5	396.3	4.6	401.6	3.9	115.4	0.5	0.00
NW10_55_3 rim	0.477	0.007	0.0634	0.0008	0.79	15.77	0.21	0.0542	0.0005	0.12	0.001	0.009	396.5	7.8	396.3	5.0	396.0	4.7	379.0	3.6	128.7	0.5	0.00
NW10_55_4	0.486	0.006	0.0637	0.0007	0.84	15.69	0.17	0.0550	0.0004	0.19	0.037	0.031	398.1	7.4	398.3	4.3	401.9	3.9	410.6	2.7	236.3	0.5	0.00
NW10_55_1_run2	0.482	0.006	0.0640	0.0008	0.93	15.62	0.31	0.0550	0.0009	0.01	0.032	0.007	399.8	7.8	399.9	4.8	399.0	4.2	410.6	6.4	446.7	4.3	0.01
NW10_55_2_run2	0.477	0.008	0.0637	0.0008	0.86	15.71	0.31	0.0547	0.0009	−0.13	<	<	397.9	7.9	397.9	5.1	395.8	5.4	398.8	6.8	138.1	1.4	0.01
NW10_55_3_run2	0.477	0.007	0.0633	0.0008	0.84	15.81	0.31	0.0549	0.0009	−0.01	0.001	0.007	395.2	7.6	395.3	4.7	396.2	4.8	409.4	6.9	153.3	1.3	0.01
NW10_55_4_run2	0.474	0.007	0.0634	0.0008	0.90	15.77	0.31	0.0545	0.0009	−0.04	<	<	396.5	7.8	396.4	5.0	394.0	4.8	391.4	6.4	193.0	1.5	0.01
NW10_55_5_run2	0.474	0.009	0.0629	0.0009	0.83	15.90	0.33	0.0544	0.0010	−0.13	0.000	0.007	393.3	8.2	393.2	5.6	393.9	6.1	389.3	7.1	88.7	1.2	0.01
NW10_55_6_run2	0.475	0.007	0.0629	0.0009	0.92	15.91	0.33	0.0549	0.0009	0.08	0.007	0.006	392.9	8.0	393.0	5.3	394.1	5.0	408.6	6.5	287.3	2.6	0.01
NW10_55_7_run2	0.478	0.010	0.0628	0.0009	0.64	15.93	0.32	0.0552	0.0013	0.09	0.002	0.009	392.2	7.9	392.5	5.2	396.2	6.8	420.3	9.5	43.0	1.6	0.04
NW10_55_8_run2	0.468	0.008	0.0623	0.0010	0.78	16.06	0.35	0.0552	0.0011	0.04	0.000	0.005	389.1	8.4	389.9	5.8	389.7	5.9	418.3	8.1	66.8	0.7	0.01
NW10_55_9_run2	0.478	0.008	0.0632	0.0009	0.87	15.84	0.32	0.0550	0.0009	0.07	0.010	0.010	394.5	8.0	394.7	5.4	395.9	5.2	412.2	6.8	160.2	2.0	0.01
NW10_55_10_run2	0.475	0.007	0.0630	0.0008	0.93	15.88	0.32	0.0551	0.0009	−0.06	0.015	0.010	393.3	7.8	393.6	5.0	394.4	4.5	415.5	6.6	418.8	3.9	0.01
NW10_55_11_run2	0.469	0.008	0.0624	0.0009	0.76	16.03	0.34	0.0548	0.0010	0.10	0.006	0.014	389.9	8.2	390.0	5.7	391.2	5.6	405.3	7.7	81.5	1.6	0.02
NW10_55_12_run2	0.476	0.012	0.0631	0.0011	0.69	15.85	0.36	0.0550	0.0013	0.03	0.000	0.005	394.2	9.0	394.4	6.5	395.9	8.1	412.2	9.7	35.9	0.7	0.02
NW10_55_13_run2	0.480	0.008	0.0634	0.0009	0.78	15.77	0.32	0.0549	0.0011	0.02	0.001	0.004	396.2	8.0	396.3	5.4	398.2	5.7	408.6	7.9	61.6	1.5	0.02
NW10_55_14_run2	0.483	0.013	0.0641	0.0010	0.68	15.60	0.34	0.0551	0.0014	−0.11	0.003	0.005	400.3	8.6	400.4	6.1	399.4	8.6	416.3	10.4	28.2	0.6	0.02
NW10_55_15_run2	0.481	0.007	0.0640	0.0009	0.92	15.62	0.32	0.0547	0.0009	0.00	0.027	0.008	400.0	8.1	399.9	5.4	398.7	5.0	399.6	6.5	391.2	3.5	0.01
NW10_55_16_run2	0.493	0.007	0.0653	0.0007	0.89	15.31	0.28	0.0549	0.0009	−0.04	<	<	407.8	7.4	407.7	4.1	406.6	4.5	407.7	6.6	181.9	1.5	0.01
NW10_55_17_run2	0.487	0.007	0.0648	0.0007	0.87	15.44	0.29	0.0544	0.0009	−0.08	0.011	0.006	404.7	7.6	404.5	4.4	402.8	4.4	388.5	6.4	177.9	1.7	0.01
NW10_55_1 core	0.477	0.003	0.0635	0.0003	0.48	15.75	0.06	0.0546	0.0009	0.10	0.013	0.008	396.8	6.2	396.8	1.5	395.9	2.3	393.8	6.4	291.0	3.4	0.01
NW10_55_2 core	0.480	0.005	0.0636	0.0003	0.33	15.73	0.06	0.0548	0.0010	0.07	0.011	0.007	397.3	6.2	397.3	1.5	398.0	3.2	405.3	7.2	123.4	1.2	0.01
NW10_55_3 core	0.483	0.003	0.0636	0.0002	0.38	15.71	0.05	0.0551	0.0009	0.13	0.004	0.010	397.5	6.1	397.7	1.2	400.3	2.1	415.5	6.7	293.6	2.7	0.01

*Results are all from zircon rims unless designated as a core analysis in the name. Where marked rim, this corresponds to a matching grain number core analysis.
*207-corrected age is calculated using Isoplot v.3.0.

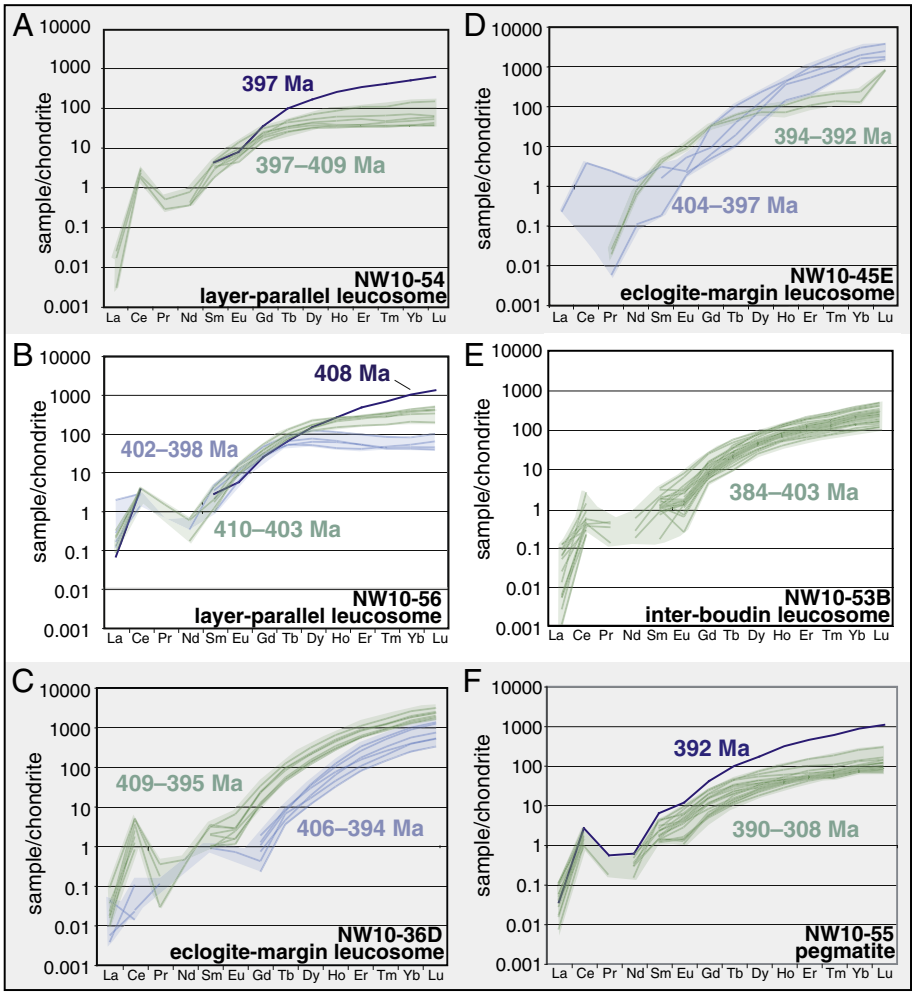

Fig. 6. REE diagrams for Scandian zircons from samples: (A) eclogite-margin leucosome NW10-36D; (B) eclogite-margin leucosome NW10-45E; (C) layer-parallel leucosome NW10-54; (D) layer-parallel leucosome NW10-56; (E) inter-boudin leucosome NW10-53B; and (F) pegmatite NW10-55. The shaded areas represent the grouped REE pattern for multiple similar analyses. Individual analyses with different REE patterns are shown as single lines. The $^{206}Pb/^{238}U$ dates that correspond to the different REE patterns are also shown.

the rims crystallized from anatectic leucosomes. Because leucosomes are complex systems in which even anatectic leucosomes do not behave exactly like larger magma bodies, the chemical and textural criteria used to interpret magmatic versus metamorphic zircons may not strictly apply. Nevertheless, we interpret the oscillatory zoning in euhedral zircons as likely indicating crystallization of Scandian zircon in the presence of melt.

In the central and northern UHP domains, the REE patterns in the Scandian zircons reveal a continuum of crystallization from high-pressure (plagioclase-absent/garnet-present) to low-pressure (plagioclase-present, garnet-absent) conditions (Fig. 6). The layer-parallel leucosomes that are transposed in the gneissic foliation yielded the oldest Scandian dates (410 Ma down to 397 Ma) (Fig. 5G,I). The trace-element analyses from these samples revealed flat, garnet-present, REE patterns and positive (NW10-56) to only slightly negative (NW10-54) Eu anomalies (Fig. 6A,B), indicative of zircon crystallization above plagioclase stability.

The texturally later leucosomes—i.e., those found along eclogite margins, the inter-boudin leucosome, and the pegmatite—revealed steeper HREE patterns and more distinct negative Eu anomalies (Fig. 6C,D,E,F). The two texturally late samples from Finnøya in the northern UHP domain revealed mainly younger dates than the layer-parallel leucosomes from the same locality, with the majority of dates from 400 to 385 Ma (Fig. 5E,F; Table 1). Also, in the northern domain, the Otrøy eclogite-margin sample (NW10-45E) yielded a mix of dates (400–390 Ma) and REE patterns, but the HREE patterns are overall steeper than those observed for the Finnøya leucosomes (Figs. 5D, 6D). Finally, the most southerly Scandian leucosome, eclogite-margin sample NW10-36D, revealed the most strongly negative Eu anomaly and a steep HREE pattern, but yielded crystallization dates that better match the layer-parallel leucosome from the north (410–395 Ma versus 410–397 Ma, respectively; Figs. 5C, 6C). These results are consistent with documented P–T–t histories for the different domains (e.g., Hacker et al., 2010).

Overall, pressure inferences from the REE patterns are consistent with the leucosome textural setting; for example, zircons from leucosomes in eclogite-boudin necks have REE patterns indicating relatively low-pressure crystallization (i.e., plagioclase-present, garnet-absent) (Fig. 6). In comparison, the layer-parallel leucosome of eclogite-hosting migmatite record a complex history with both plagioclase-present/garnet-present (NW10-54) and plagioclase-absent/garnet-present (NW10-56) REE patterns displayed by leucosomes from the same outcrop (Fig. 6).

Based on experimental results and thermodynamic calculations, Labrousse et al. (2011) concluded that initial partial melting within the WGR occurred at the peak conditions recorded by the eclogite. However, because plagioclase is abundant in the WGR leucosomes and appears to have crystallized on the solidus, final melt crystallization likely took place below 15–20 kbar (i.e., where plagioclase becomes stable, Patiño Douce and McCarthy, 1998). Based on the whole-rock

Table 2
Rare-earth element data normalized to chondrite for zircons from Western Gneiss Region crystallized melt.

Sample, grain number	La	Ce	Pr	Nd	Sm	Eu	Gd	Tb	Dy	Ho	Er	Tm	Yb	Lu	Hf	Eu*[a,b]	Lu/Dy
NW10-54, layer-parallel leucosome (*UTM*: *371945, 6965140*)																	
NW10_54_1	0.00	0.95	0.00	0.00	4.26	7.71	34.5	95.9	162.4	251.1	332.5	399.6	489.5	596.7	143506	−0.20	2.4
NW10_54_2	0.00	2.92	0.00	0.00	4.65	9.89	20.9	32.3	38.4	36.3	36.0	37.3	38.0	44.2	119645	0.00	1.2
NW10_54_3	0.00	3.83	0.00	0.00	3.32	5.05	18.5	31.0	44.4	56.1	76.9	98.3	155.0	213.8	119242	−0.19	3.8
NW10_54_4	0.02	1.71	0.00	0.00	3.80	7.79	28.4	49.5	70.1	91.0	111.3	126.2	168.9	197.8	112610	−0.12	2.2
NW10_54_5	0.02	2.45	0.00	0.43	4.86	14.35	32.1	45.2	54.6	63.5	65.1	68.0	73.2	65.9	117613	0.06	1.0
NW10_54_6	0.00	1.86	0.00	0.00	3.55	4.55	15.4	25.9	34.0	38.0	39.3	45.5	49.6	55.1	116543	−0.21	1.4
NW10_54_7	0.03	0.31	0.00	0.00	1.57	2.34	16.4	35.4	63.3	97.0	129.8	147.2	187.2	215.2	113057	−0.34	2.2
NW10_54_8	0.00	0.47	0.00	0.00	1.69	3.58	10.0	33.9	62.1	91.9	127.4	147.3	203.4	244.5	118279	−0.06	2.7
NW10_54_9	0.00	2.66	0.00	0.00	3.20	6.42	19.0	27.0	32.7	33.7	35.8	35.1	38.5	38.3	122719	−0.08	1.1
NW10_54_10	0.00	2.02	0.52	0.80	4.17	7.09	25.8	34.6	45.4	49.8	55.6	49.0	57.1	62.6	128543	−0.17	1.3
NW10_54_11	0.03	3.15	0.00	0.36	3.00	8.61	24.5	35.7	43.9	39.5	39.1	37.4	38.2	38.3	116015	0.00	1.0
NW10_54_12	0.01	3.14	0.29	0.00	8.08	14.09	35.5	57.2	81.9	97.2	107.7	121.2	149.7	189.8	120890	−0.08	2.0
NW10_54_13	0.00	1.79	0.28	0.35	1.76	5.67	20.5	48.1	68.2	84.3	105.4	106.0	136.8	145.2	115216	−0.03	1.7
NW10_54_14	0.00	2.12	0.00	0.00	3.59	4.56	9.8	21.3	30.1	35.7	52.6	74.2	93.5	110.2	119398	−0.11	3.1
NW10_54_1 core	0.04	0.62	0.00	0.00	2.90	4.24	26.4	68.0	116.1	176.3	237.7	274.5	356.3	437.9	111216	−0.31	2.5
NW10_54_2 core	0.02	2.99	0.00	0.38	5.44	10.80	26.3	36.6	43.1	41.7	42.9	39.5	45.8	38.7	102630	−0.04	0.9
NW10_54_3 core	0.09	34.41	0.78	3.55	29.19	20.11	102.1	163.9	279.0	486.7	844.0	1189.0	1761.9	2313.0	85445	−0.43	4.8
NW10_54_4 core	0.33	122.62	4.44	18.72	94.40	50.61	275.3	448.5	704.2	1076.3	1689.1	2205.0	3290.7	3696.2	86247	−0.50	3.4
NW10_54_5 core	0.08	2.76	0.00	0.31	2.53	6.80	15.7	25.0	26.1	29.1	26.0	22.6	28.2	26.3	110415	0.03	0.9
NW10_54_6 core	<	0.75	0.00	0.00	0.00	1.56	9.0	23.0	41.6	76.3	117.2	157.2	206.1	270.8	110535	<	3.6
NW10_54_7 core	0.03	1.77	0.00	0.00	1.38	5.86	12.5	37.0	62.8	96.4	114.7	122.5	182.3	187.5	109729	0.15	1.9
NW10_54_8 core	0.02	2.34	0.00	0.00	5.60	10.45	30.5	40.3	51.1	47.3	49.7	37.5	47.6	43.1	108132	−0.10	0.9
NW10_54_9 core	<	21.36	0.33	0.58	1.99	4.10	21.0	39.2	75.5	160.6	307.7	483.2	932.2	1392.9	89264	−0.20	8.7
NW10_54_10 core	<	13.02	0.00	0.23	4.34	2.65	19.8	43.5	90.3	179.8	334.2	602.8	1070.8	1456.6	109441	−0.54	8.1
NW10-56, layer-parallel leucosome (*UTM*: *371945, 6965140*)																	
NW10_56_1	1.16	1.67	0.00	<	1.19	5.11	14.9	31.3	30.4	25.5	24.2	27.6	31.1	37.9	98517	0.08	1.2
NW10_56_2	0.61	27.56	0.00	0.15	1.16	2.35	19.9	33.8	70.5	145.5	263.8	431.6	776.1	1151.5	90616	−0.31	16.3
NW10_56_4	0.64	0.88	0.26	<	0.58	5.79	14.1	30.6	29.3	26.9	19.5	20.4	20.2	18.9	111891	0.31	0.6
NW10_56_5	0.38	1.11	0.00	<	0.00	2.06	8.3	18.0	27.2	32.6	35.4	39.5	45.6	43.3	98654	<	1.6
NW10_56_6	0.13	1.87	0.00	<	1.24	5.55	23.3	58.6	101.0	155.1	167.9	201.1	232.3	252.3	106596	0.01	2.5
NW10_56_8	0.17	19.23	0.65	0.84	10.26	9.41	41.5	69.3	119.1	229.3	356.2	482.8	770.9	1039.6	81034	−0.34	8.7
NW10_56_10	0.19	1.99	0.00	<	0.56	7.37	18.6	50.5	84.5	125.5	145.6	179.4	226.2	251.2	97495	0.36	3.0
NW10_56_11	0.13	2.06	0.00	0.10	0.71	5.45	14.6	43.7	84.8	130.5	172.4	199.6	254.2	295.8	107831	0.23	3.5
NW10_56_12	0.07	1.81	0.00	0.20	2.71	9.41	27.5	52.4	72.9	66.4	57.0	49.4	48.2	59.1	105933	0.04	0.8
NW10_56_13	0.11	22.19	0.00	0.26	1.97	4.71	19.4	47.7	96.2	190.8	378.5	614.5	1054.9	1689.7	93216	−0.12	17.6
NW10_56_14	0.16	1.65	0.00	<	2.04	6.65	18.4	30.5	37.1	36.1	31.5	26.1	26.9	26.7	107268	0.03	0.7
NW10_56_15	0.07	3.65	0.00	<	2.80	5.62	25.0	64.2	147.1	264.8	475.3	673.3	1015.5	1315.7	117792	−0.17	8.9
NW10_56_16	0.12	2.20	0.00	<	1.02	5.58	18.3	44.7	72.2	88.3	97.3	102.5	122.0	117.3	107494	0.11	1.6
NW10_56_17	0.07	2.36	0.88	0.35	1.21	9.83	31.5	76.5	130.9	154.9	163.6	166.9	191.0	199.8	107907	0.20	1.5
NW10_56_18	0.10	0.83	0.00	<	0.55	3.60	17.1	38.5	44.8	39.0	31.0	24.8	24.6	23.4	113340	0.07	0.5
NW10_56_19	0.07	1.88	0.00	0.23	0.00	6.64	17.7	39.4	52.0	59.3	62.2	70.0	81.6	87.7	101394	<	1.7
NW10_56_20	0.05	2.45	0.00	0.38	2.53	9.03	22.0	57.7	100.8	137.9	154.9	160.8	216.0	240.5	101168	0.08	2.4
NW10_56_1 core	0.02	30.21	0.56	0.80	5.25	5.54	22.2	45.7	88.7	172.2	331.3	490.3	847.6	1223.8	90395	−0.29	13.8
NW10_56_2 core	0.07	2.58	0.00	0.00	3.96	5.82	22.2	59.4	109.0	167.4	222.7	263.3	323.4	367.6	104211	−0.21	3.4
NW10_56_3 core	0.07	2.27	0.00	0.48	4.05	9.32	31.5	90.7	160.0	236.0	300.5	355.7	464.7	485.4	102567	−0.08	3.0
NW10_56_4 core	0.34	12.53	2.31	2.00	9.58	14.66	50.2	85.8	162.2	260.4	406.2	513.0	719.7	914.2	86351	−0.17	5.6
NW10_56_5 core	<	6.24	0.00	0.00	3.56	4.94	21.7	40.5	68.4	116.6	172.6	252.2	428.2	609.8	102636	−0.25	8.9
NW10_56_6 core	<	31.82	21.89	15.31	63.80	67.73	223.8	296.5	462.1	737.5	1092.3	1437.7	1955.0	2298.5	67312	−0.25	5.0
NW10_56_7 core	<	1.78	0.00	0.00	1.70	5.31	17.4	37.6	79.1	118.5	149.0	195.4	243.8	247.0	98515	−0.01	3.1
NW10-36D, eclogite margin leucosome (*UTM*: *325810, 6920646*)																	
NW10_36D_2 rim	0.00	<	0.00	0.23	1.03	0.00	0.3	4.8	19.6	61.7	162.0	331.6	624.7	866.5	127417	<	44.2
NW10_36D_3 rim	0.01	2.72	0.00	0.00	2.07	1.62	12.2	51.5	144.0	318.4	616.0	992.7	1640.7	2176.9	133319	−0.49	15.1
NW10_36D_4 rim	<	0.35	0.00	0.00	0.97	0.76	0.4	7.1	17.7	48.8	115.6	218.8	422.1	576.2	138558	0.06	32.6
NW10_36D_5 rim	0.05	0.01	0.00	0.00	0.00	0.00	2.0	8.6	36.5	111.6	279.6	547.8	963.2	1371.0	122399	<	37.6
NW10_36D_6 rim	0.00	0.11	0.00	0.00	0.00	0.00	1.3	9.7	31.6	82.4	167.0	279.1	425.9	567.3	125947	<	18.0
NW10_36D_7	0.01	10.61	0.00	0.00	2.99	3.60	13.0	18.9	26.8	33.3	51.5	74.8	111.6	147.4	103795	−0.24	5.5
NW10_36D_8	0.13	48.67	1.31	4.09	27.39	21.10	115.1	246.4	551.5	1232.9	2226.9	3236.3	5152.1	6848.3	87373	−0.42	12.4
NW10_36D_9	0.04	1.33	0.00	0.00	1.12	1.20	13.6	53.5	145.9	321.8	611.3	920.4	1389.3	1774.2	134016	−0.51	12.2
NW10_36D_10	0.02	1.91	0.00	0.00	1.05	1.68	11.6	47.5	126.9	298.6	606.4	978.1	1522.1	2025.7	140856	−0.32	16.0
NW10_36D_11	0.09	5.25	0.37	0.49	3.29	6.92	36.0	133.2	334.3	701.2	1197.9	1806.2	2810.5	3417.7	128128	−0.20	10.2
NW10_36D_12	0.02	0.89	0.00	0.00	0.93	2.59	12.9	58.7	164.3	371.3	671.3	1022.4	1438.4	1888.3	134010	−0.12	11.5
NW10_36D_13	<	3.96	0.03	0.37	3.76	3.02	24.4	101.9	228.4	507.5	912.8	1328.6	1994.9	2534.3	135899	−0.50	11.1
NW10_36D_14	0.02	5.48	0.18	0.00	2.16	2.85	25.6	103.6	243.0	541.2	960.6	1330.4	2131.2	2727.8	142996	−0.42	11.2
NW10_36D_15	<	2.93	0.00	0.00	3.17	1.24	14.4	47.1	109.6	267.4	539.3	900.6	1526.9	1997.6	126071	−0.74	18.2
NW10_36D_16	<	<	0.00	0.00	0.00	0.00	0.8	4.9	20.6	69.6	187.0	354.9	606.0	813.3	120734	<	39.5
NW10_36D_17	<	2.28	0.00	0.33	1.25	1.74	8.3	21.8	42.1	98.0	198.0	328.5	578.1	908.3	118192	−0.27	21.6
NW10_36D_18	0.01	0.02	0.00	0.00	0.00	0.00	0.2	3.9	12.4	34.6	87.2	156.1	269.3	358.3	128301	<	28.8
NW10_36D_19	<	0.03	0.12	0.00	0.00	0.00	1.1	8.2	38.8	133.6	356.3	634.7	1083.5	1471.5	133200	<	37.9
NW10_36D_20	0.04	12.77	0.28	0.65	11.78	10.16	78.9	274.1	607.6	1256.8	2361.2	3418.6	5455.2	7071.2	138220	−0.48	11.6
NW10_36D_21	0.02	3.80	0.00	0.00	3.36	3.09	24.5	89.1	229.8	481.6	897.0	1311.0	1982.3	2599.9	133429	−0.47	11.3
NW10_36D_1 core	0.03	3.63	0.00	0.44	2.07	2.90	13.6	27.7	46.5	61.2	76.9	93.4	146.1	229.7	113160	−0.26	21.9

(continued on next page)

Table 2 (*continued*)

Sample, grain number	La	Ce	Pr	Nd	Sm	Eu	Gd	Tb	Dy	Ho	Er	Tm	Yb	Lu	Hf	Eu*[a,b]	Lu/Dy
NW10-36D, eclogite margin leucosome (*UTM*: *325810, 6920646*)																	
NW10_36D_2 core	0.04	5.96	0.00	0.90	3.39	5.52	16.6	21.5	25.4	27.8	27.2	30.4	40.8	40.6	118853	−0.13	1.6
NW10_36D_3 core	0.05	6.03	0.00	0.00	2.13	4.80	18.4	32.8	44.1	56.8	70.1	96.3	179.6	225.6	119526	−0.12	5.1
NW10_36D_4 core	<	0.05	0.00	0.00	0.00	0.00	2.1	18.3	51.3	126.0	282.8	523.3	913.3	1167.7	111582	<	22.8
NW10_36D_5 core	0.03	0.04	0.00	0.18	0.00	0.00	4.8	20.3	70.4	193.3	406.0	737.8	1237.7	1612.9	122199	<	22.9
NW10_36D_6 core	0.03	0.00	0.00	0.00	0.00	0.00	1.3	8.5	32.2	111.6	308.5	624.2	1134.2	1523.0	125058	<	47.4
NW10-45E, eclogite margin leucosome (*UTM*: *383738, 6958619*)																	
NW10_45E_1	15.52	73.74	96.00	42.24	41.55	29.12	43.8	78.6	136.0	231.7	415.1	837.2	1830.3	3076.1	142423	−0.17	22.6
NW10_45E_2	0.30	65.29	28.37	34.93	103.65	74.77	184.7	221.6	280.5	355.4	507.7	802.9	1479.1	2234.2	131848	−0.27	8.0
NW10_45E_3	0.05	37.80	3.18	6.86	33.46	26.58	92.1	122.3	157.8	213.4	303.8	516.4	1017.0	1622.5	113369	−0.32	10.3
NW10_45E_4	0.23	1.85	2.87	1.21	4.18	5.92	17.4	34.3	45.0	60.3	75.5	85.0	114.6	100.8	104328	−0.16	2.2
NW10_45E_5	0.02	0.02	0.00	<	<	0.00	0.7	4.3	19.0	66.4	237.5	700.7	1885.9	3372.8	179814	<	177.6
NW10_45E_6	4.14	15.51	48.08	20.53	31.66	17.42	45.5	69.7	107.9	170.2	280.1	432.2	684.1	858.1	131054	−0.34	7.9
NW10_45E_8	0.05	0.75	0.00	<	1.45	4.79	8.6	36.6	121.3	389.7	918.7	1656.7	2788.5	3481.7	194332	0.13	28.7
NW10_45E_9	0.21	3.51	2.20	1.22	2.84	2.17	30.0	96.8	212.1	414.0	689.5	1112.8	1817.6	2304.7	130031	−0.63	10.9
NW10_45E_10	<	0.56	0.00	<	1.53	1.39	16.7	62.7	151.3	316.1	514.4	853.5	1455.9	1993.1	116410	−0.56	13.2
NW10_45E_1_run2	0.00	0.00	0.02	0.54	3.56	10.38	31.0	57.0	84.8	102.0	159.7	195.9	219.1	774.3	106689	−0.01	9.1
NW10_45E_2_run2	0.00	0.00	0.02	0.72	4.24	8.22	29.7	44.5	66.9	65.9	99.9	127.0	120.0	754.7	105263	−0.14	11.3
NW10_45E_4_run2	0.00	0.00	0.01	0.09	0.00	1.99	4.5	9.8	39.3	133.0	197.4	437.2	1091.2	1443.8	189297	<	36.7
NW10_45E_5_run2	0.00	0.00	0.00	0.10	0.17	1.69	5.8	17.9	79.1	333.2	496.2	790.3	1509.7	1637.5	212927	0.24	20.7
NW10-53B, inter-boudin leucosome (*UTM*: *371945, 6965140*)																	
NW10_53b_1	<	0.25	0.00	0.00	0.00	2.16	11.7	25.7	43.9	60.7	82.3	102.7	123.9	131.1	99073	<	3.0
NW10_53b_2	−0.01	0.30	0.00	0.00	0.91	0.23	4.2	8.6	22.7	36.4	52.5	68.7	85.8	109.6	120062	−0.93	4.8
NW10_53b_3	0.00	0.33	0.00	0.00	0.76	<	6.0	17.4	42.1	77.9	113.9	150.7	204.2	266.0	112405	<	6.3
NW10_53b_4	<	0.46	0.00	0.00	1.09	1.12	9.4	22.5	52.0	87.9	129.4	165.2	229.1	250.4	115951	−0.46	4.8
NW10_53b_5	0.00	0.21	0.00	0.00	0.15	1.18	5.3	13.4	29.6	52.7	76.0	101.4	129.3	169.6	113320	0.12	5.7
NW10_53b_6	0.00	0.34	0.00	0.00	0.00	0.98	6.7	21.3	42.5	67.9	110.0	128.2	186.5	225.8	116782	<	5.3
NW10_53b_7	0.00	0.34	0.00	0.00	1.12	1.37	6.5	18.1	44.3	74.9	113.6	140.2	188.8	221.6	118850	−0.29	5.0
NW10_53b_8	0.01	0.32	0.00	0.25	0.00	1.10	6.5	19.1	41.5	66.7	94.2	123.0	159.7	203.8	113787	<	4.9
NW10_53b_9	0.01	0.20	0.00	0.00	0.90	1.51	6.2	16.3	30.0	47.7	72.7	97.9	129.7	147.7	112798	−0.19	4.9
NW10_53b_10	<	0.39	0.00	0.17	0.77	1.17	8.5	17.7	39.3	63.3	95.7	121.2	168.4	208.5	113017	−0.34	5.3
NW10_53b_11	<	0.09	0.00	0.00	1.03	0.57	6.2	15.5	37.9	67.8	115.4	152.7	214.2	268.6	107514	−0.65	7.1
NW10_53b_12	0.01	0.38	0.12	0.00	0.93	2.43	7.5	20.5	39.0	64.1	102.8	127.7	191.1	233.9	107700	−0.03	6.0
NW10_53b_13	0.00	0.55	0.00	0.25	1.66	1.56	7.3	37.6	69.1	111.1	169.5	221.3	299.7	372.7	111487	−0.35	5.4
NW10_53b_14	0.00	0.43	0.00	0.00	1.02	1.22	7.6	21.4	43.0	76.8	124.5	165.0	239.7	290.7	108513	−0.36	6.8
NW10_53b_15	<	0.33	0.31	0.00	1.37	1.39	14.3	32.9	70.1	122.7	196.0	250.7	355.0	452.6	115628	−0.50	6.5
NW10_53B_1_run2	<	0.47	0.00	0.00	1.56	0.64	6.9	18.7	35.5	63.1	87.9	112.9	147.0	179.2	113110	−0.71	5.0
NW10_53B_2_run2	<	2.14	0.00	0.00	3.00	7.22	24.0	52.4	79.4	113.3	145.4	171.2	249.3	313.4	100924	−0.07	3.9
NW10_53B_3_run2	0.17	22.72	6.56	5.42	17.62	25.50	53.7	101.8	174.7	320.3	515.5	750.5	1326.4	1893.9	99652	−0.08	10.8
NW10_53B_4_run2	<	0.45	0.00	0.00	1.78	2.24	14.1	31.4	50.5	76.2	89.2	95.6	128.8	149.5	106614	−0.35	3.0
NW10_53B_5_run2	0.12	0.26	0.00	0.00	0.77	1.15	10.8	21.1	36.2	48.7	60.7	83.5	88.0	106.9	105610	−0.40	3.0
NW10_53B_6_run2	0.23	5.98	1.12	0.00	3.17	4.15	15.7	31.5	70.4	120.1	183.3	280.9	438.9	632.0	107261	−0.23	9.0
NW10_53B_7_run2	0.09	81.55	2.08	3.98	24.53	12.62	108.5	189.7	377.5	699.6	1083.9	1574.4	2320.1	2959.8	96653	−0.61	7.8
NW10_53B_8_run2	<	0.56	0.00	0.00	0.95	1.16	7.7	18.2	41.6	69.3	106.7	134.3	193.3	232.6	124425	−0.37	5.6
NW10_53B_9_run2	0.08	0.41	0.00	0.50	0.00	1.12	5.3	14.8	28.2	49.9	66.5	90.8	123.8	156.1	115233	<	5.5
NW10_53B_13_run2	0.06	0.79	0.00	0.00	1.63	1.43	9.5	31.8	71.0	125.7	176.3	230.2	328.9	443.9	117553	−0.44	6.3
NW10_53B_14_run2	53.73	224.46	170.23	219.32	228.12	173.13	310.3	361.1	492.0	766.6	1162.8	1800.1	2911.2	4146.7	106032	−0.19	8.4
NW10_53B_15_run2	0.11	0.50	0.38	0.00	1.56	3.00	13.2	31.2	76.5	120.6	177.6	225.0	315.3	406.9	117315	−0.18	5.3
NW10_53B_16_run2	0.01	2.41	0.00	0.52	1.88	5.81	22.8	43.8	69.5	93.5	115.0	148.6	221.6	283.5	109755	−0.05	4.1
NW10_53B_17_run2	0.13	22.21	0.88	0.55	5.20	5.40	28.2	60.9	140.3	266.9	470.3	757.9	1407.4	1863.1	106055	−0.35	13.3
NW10_53B_18_run2	0.05	0.27	0.00	0.33	0.00	0.77	5.5	11.2	26.0	46.8	58.9	70.9	101.5	120.3	111868	<	4.6
NW10_53B_19_run2	0.08	1.25	0.00	0.00	2.79	2.66	13.6	18.5	36.9	59.1	83.6	117.3	200.6	270.7	109997	−0.36	7.3
NW10_53B_20_run2	0.02	0.37	0.42	0.00	1.12	2.79	7.5	25.3	59.2	109.1	169.0	202.9	298.7	382.8	113154	−0.02	6.5
NW10_53B_21_run2	<	0.38	0.00	0.00	0.64	1.37	8.0	18.7	39.1	64.5	87.2	114.5	161.3	195.8	106331	−0.22	5.0
NW10_53B_22_run2	<	0.37	0.00	0.00	1.06	3.60	11.2	25.5	48.8	74.5	104.3	113.3	175.7	210.6	116262	0.02	4.3
NW10-55, pegmatite (*UTM*: *371945, 6965140*)																	
NW10_55_1	0.01	0.94	0.00	0.00	1.35	1.17	6.4	13.4	22.6	34.5	49.6	68.4	91.6	116.1	113392	−0.40	5.1
NW10_55_2	0.04	2.63	0.54	0.60	6.29	11.68	40.9	98.0	168.2	308.5	447.1	593.0	864.6	1070.6	119077	−0.14	6.4
NW10_55_3	0.01	1.37	0.00	0.27	1.32	4.46	10.0	18.6	27.4	37.0	48.9	58.3	80.6	97.7	113457	0.09	3.6
NW10_55_4	<	1.74	0.00	0.14	4.07	5.53	14.6	30.9	34.7	42.4	52.7	55.5	73.7	76.2	115766	−0.14	2.2
NW10_55_1_run2	0.10	2.52	0.00	0.43	3.69	8.76	22.7	41.9	51.5	57.0	64.0	66.5	86.0	90.1	112413	−0.02	1.7
NW10_55_2_run2	0.10	1.62	0.00	0.00	2.46	7.50	24.1	44.3	58.8	76.2	96.3	103.5	132.2	158.1	109640	−0.01	2.7
NW10_55_3_run2	0.02	1.60	0.00	0.00	1.66	3.28	11.2	18.7	30.5	37.6	47.6	55.8	71.8	87.9	109498	−0.12	2.9
NW10_55_4_run2	0.10	1.69	0.00	0.00	1.26	2.62	10.5	21.1	31.5	37.3	44.4	58.1	71.6	78.5	108692	−0.14	2.5
NW10_55_5_run2	0.04	1.08	0.00	0.00	1.16	1.50	4.6	10.1	16.8	26.6	40.2	51.9	70.9	87.5	109033	−0.19	5.2
NW10_55_6_run2	0.10	1.88	0.00	0.00	2.17	3.74	14.5	28.1	34.0	43.3	51.8	46.7	67.7	68.8	111580	−0.18	2.0
NW10_55_7_run2	0.04	1.36	0.00	0.54	2.03	5.52	18.7	41.7	69.7	101.6	142.6	175.9	242.8	288.0	109141	−0.05	4.1
NW10_55_8_run2	0.03	1.25	0.00	0.31	0.00	0.98	5.4	12.0	25.0	37.5	59.3	74.7	100.2	135.1	115527	<	5.4
NW10_55_9_run2	0.04	1.29	0.00	0.00	1.53	3.60	7.8	14.5	24.5	33.5	42.8	55.6	69.0	79.5	109526	0.02	3.2
NW10_55_10_run2	0.09	2.05	0.00	0.27	3.82	5.97	18.2	29.9	40.5	42.0	45.9	47.9	66.1	65.4	112390	−0.15	1.6
NW10_55_11_run2	<	1.01	0.00	0.31	1.30	1.31	5.2	11.3	20.5	31.8	50.1	63.4	82.3	98.6	110159	−0.30	4.8
NW10_55_12_run2	0.00	0.77	0.00	0.00	1.09	1.31	5.3	13.4	23.9	36.7	54.8	68.0	95.9	115.5	106910	−0.27	4.8
NW10_55_13_run2	0.09	0.91	0.17	0.00	1.25	1.32	4.9	11.3	21.4	34.3	50.3	67.5	99.3	114.6	110979	−0.27	5.4
NW10_55_14_run2	0.03	0.82	0.00	0.00	0.00	1.24	5.1	17.0	30.8	49.9	72.8	85.5	126.5	138.1	111157	<	4.5

Table 2 (*continued*)

Sample, grain number	La	Ce	Pr	Nd	Sm	Eu	Gd	Tb	Dy	Ho	Er	Tm	Yb	Lu	Hf	Eu*[a,b]	Lu/Dy
NW10-55, pegmatite (*UTM: 371945, 6965140*)																	
NW10_55_15_run2	0.05	2.10	0.00	0.33	2.13	4.21	15.3	31.8	41.3	48.7	52.1	53.8	69.1	72.6	111563	−0.13	1.8
NW10_55_16_run2	0.05	1.58	0.00	0.00	2.89	3.78	10.7	22.0	27.0	39.2	48.0	49.8	71.5	78.1	113563	−0.17	2.9
NW10_55_17_run2	0.02	1.50	0.00	0.00	1.54	4.70	14.6	24.6	34.6	42.7	52.0	58.7	80.4	88.4	110820	0.00	2.6
NW10_55_1 core	0.07	2.01	0.00	0.00	5.23	9.20	29.7	49.9	61.9	71.9	82.7	87.1	106.7	112.3	112009	−0.13	1.8
NW10_55_2 core	<	1.08	0.00	0.22	4.58	7.61	19.3	27.4	30.4	33.8	32.1	34.3	41.7	45.1	94158	−0.09	1.5
NW10_55_3 core	<	1.80	0.00	0.54	7.69	16.86	41.0	67.7	90.0	105.6	123.1	126.6	171.7	175.8	110777	−0.02	2.0

[a] $Eu^* = Log(Eu) - ((Log(Gd) + Log(Sm))/2)$.
[b] ≤ values are below the detection limit.

compositional results from representative leucosomes (Fig. 7; Table 3), the euhedral crystal morphology and oscillatory and sector-zoned texture of zircon rims from these leucosomes (Fig. 4), and their trace-element signatures that generally indicate garnet-present and high-pressure plagioclase-absent conditions (Fig. 6), we interpret our U–Pb age results from leucosome zircons to record the transition from high-P (garnet-present) conditions (ca. 410–400 Ma) to lower-P (plagioclase-present) conditions (ca. 400–385 Ma) in the northern UHP domain.

The leucosome crystallization dates ranging from ~410 to 400 Ma are similar to UHP metamorphic ages determined by a variety of isotopic systems and analytical techniques applied to garnet and/or zircon in nearby eclogite in the central and northern UHP domains (Fig. 8; Krogh et al., 2004, 2011; Kylander-Clark et al., 2007; Mørk and Mearns, 1986). In addition, texturally late leucosomes (including a cross-cutting pegmatite dike) yielded similar dates (400–385 Ma) to the lower pressure, amphibolite-facies (1.5–0.5 GPa) overprint that affected many eclogite bodies (Krogh et al., 2011; Kylander-Clark et al., 2008; Terry et al., 2000b; Walsh et al., 2007).

7.2. Implications for subduction dynamics

Our results show that zircon crystallization in layer-parallel leucosome in the eclogite-hosting migmatite (410–400 Ma) overlapped with UHP eclogite metamorphism of the WGR (425–400 Ma) (Fig. 8). Although our results do not indicate when partial melting started, and we cannot determine the exact pressure of zircon crystallization (only

Table 3
Bulk-rock compositions and trace-element data for Western Gneiss Region leucosomes and pegmatite.

Sample number	NW10-06	NW10-12	NW10-36D	NW10-36E	NW10-45E	NW10-50	NW10-54	NW10-55	NW10-56
Major elements (*wt.%*; *XRF*)									
SiO_2	75.04	62.85	69.99	73.75	71.75	71.80	65.61	63.45	68.61
TiO_2	0.08	0.01	0.27	0.05	0.03	0.11	0.58	0.56	0.29
Al_2O_3	13.18	23.28	15.45	14.77	16.35	14.36	16.37	17.47	15.49
FeO	0.58	0.06	2.41	0.40	0.71	0.85	4.16	4.62	2.00
MnO	0.01	0.00	0.07	0.01	0.03	0.03	0.09	0.08	0.05
MgO	0.23	0.00	1.20	0.12	0.36	0.27	2.01	2.56	0.93
CaO	1.77	4.41	3.06	1.20	3.38	1.54	3.86	3.46	2.53
Na_2O	2.87	8.92	4.13	3.07	5.43	2.99	3.84	5.05	3.19
K_2O	4.34	0.23	1.88	5.32	0.80	5.42	2.35	2.04	5.03
P_2O_5	0.02	0.00	0.06	0.04	0.01	0.05	0.18	0.04	0.09
Sum	98.13	99.76	98.51	98.74	98.86	97.42	99.05	99.33	98.20
LOI (%)	0.31	0.54	0.34	0.54	0.30	0.59	0.50	0.41	0.35
Trace elements (*ppm*; *ICP–MS*)									
La	8.5	0.1	41.7	6.6	27.6	39.6	31.5	0.7	34.1
Ce	16.1	0.2	85.8	11.8	48.8	77.1	61.6	1.4	67.1
Pr	1.9	<	9.8	1.4	5.4	8.5	7.2	0.2	7.8
Nd	6.9	0.1	36.1	4.9	19.5	29.7	26.9	0.8	29.4
Sm	1.3	<	6.6	1.0	3.8	5.3	4.8	0.3	5.1
Eu	0.6	<	1.4	0.8	1.6	1.2	1.4	0.2	1.3
Gd	1.0	<	5.4	0.7	2.5	3.7	3.9	0.9	3.8
Tb	0.2	<	0.8	0.1	0.4	0.5	0.6	0.2	0.6
Dy	0.9	<	4.6	0.6	2.7	2.4	3.7	1.7	3.3
Ho	0.2	<	0.9	0.1	0.6	0.4	0.8	0.4	0.7
Er	0.5	<	2.4	0.3	1.6	0.8	2.0	1.3	1.9
Tm	0.1	<	0.4	<	0.2	0.1	0.3	0.2	0.3
Yb	0.5	<	2.1	0.2	1.2	0.6	1.8	1.2	1.7
Lu	0.1	<	0.3	<	0.2	0.1	0.3	0.2	0.3
Ba	1037.0	114.0	432.0	687.0	97.0	1055.0	778.0	463.0	1950.0
Th	2.4	<	16.3	2.4	7.2	20.5	5.4	0.1	5.6
Nb	2.1	<	8.9	3.3	0.1	3.9	7.4	8.1	6.3
Y	5.2	0.1	23.4	2.5	14.3	9.5	20.1	10.5	17.1
Hf	1.3	<	2.7	1.6	0.2	2.3	3.9	0.8	5.6
Ta	0.1	<	0.9	0.3	<	0.3	0.4	0.3	0.4
U	0.4	<	2.6	0.7	1.7	1.5	0.8	0.1	0.7
Pb	23.1	14.4	31.3	50.2	26.6	41.2	10.3	10.0	15.4
Rb	105.4	1.5	70.7	125.6	6.6	101.7	61.8	74.3	90.3
Cs	2.5	0.1	2.2	1.6	0.2	1.5	0.9	2.1	0.4
Sr	306.0	392.0	363.0	262.0	1118.0	264.0	483.0	496.0	526.0
Sc	1.8	0.1	4.5	1.8	2.0	2.4	10.3	14.7	4.7
Zr	37.0	0.0	94.0	41.0	4.0	72.0	156.0	29.0	236.0

Analyses done using the XRF and the ICP–MS at Washington State University (Johnson et al., 1999).

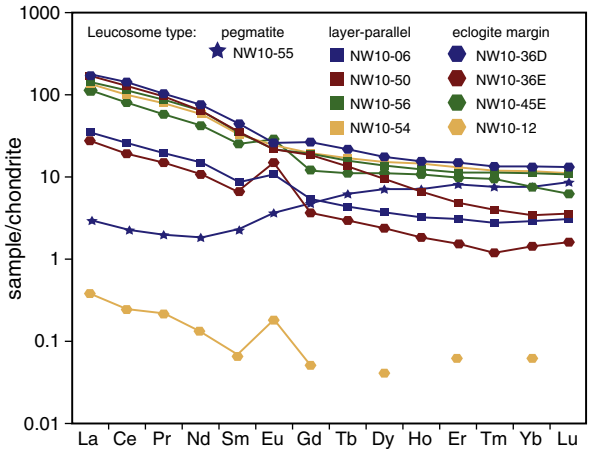

Fig. 7. REE diagrams for the bulk composition of the leucosomes. The REE results are keyed by textural type (i.e., layer-parallel leucosome, eclogite-margin leucosome or pegmatite) and by sample number.

whether plagioclase and garnet were likely present or absent), these zircon data show that partial melt was likely present during Scandian UHP metamorphism and certainly during initial decompression.

The rheological implications for the existence of partial melt at high pressure must be considered for the processes of exhumation of (U)HP rocks in the WGR and in other UHP terranes that expose abundant migmatite in association with eclogite. The presence of partial melt (melt fraction > 10–15%) dramatically decreases viscosity. This reduces material strength at the interface between subducted crust and overlying plate and may trigger the switch between continental subduction and exhumation of UHP crustal material. If present in significant quantities, melt initiates a dynamic instability that drives upward flow of partially molten crust and can rapidly ferry dense, unmelted fragments towards the Earth's surface (Labrousse et al., 2011). Alternatively, a tectonic switch driving decompression could trigger partial melting, with subsequent feedbacks between decompression and melting. The new geochronometric and trace-element data from the central and northern UHP domains support the idea that migmatization occurred at high-P conditions and could have dramatically affected the rheology of the WGR crust during continental subduction and exhumation.

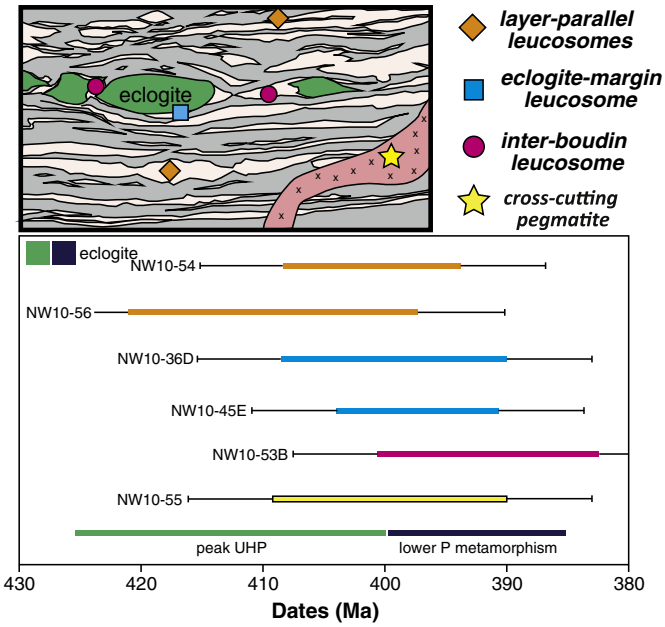

Fig. 8. Sample versus age plot for all leucosomes studied and cartoon diagram of the different textural types of leucosomes. Bars on the range of dates reveal the 2 sigma errors. The timing of peak UHP metamorphism and the lower-pressure retrogression event are also shown for reference. Note that the range of dates from all of the leucosomes overlap in part with the timing of UHP metamorphism throughout the Western Gneiss Region. See text for studies used to define the timing of peak UHP metamorphism and lower pressure metamorphism.

Supplementary data to this article can be found online at http://dx.doi.org/10.1016/j.lithos.2013.02.003.

Acknowledgments

This research was funded by NSF grants EAR-1062187 to S.M. Gordon and EAR-1040980 to D.L. Whitney and C. Teyssier. We thank B. Hacker and A. Kylander-Clark for many fruitful discussions and for their help in the ICPMS laboratory at the University of California, Santa Barbara. In addition, sample collection and discussions with Roxanne Renedo contributed to this work. This manuscript also greatly benefited from two anonymous reviewers.

References

Auzanneau, E., Vielzeuf, D., Schmidt, M.W., 2006. Experimental evidence of decompression melting during exhumation of subducted continental crust. Contributions to Mineralogy and Petrology 152, 125–148.
Beyer, E.E., Brueckner, H.K., Griffin, W.L., O'Reilly, S.Y., 2012. Laurentian provenance of Archean mantle fragments in the Proterozoic Baltic crust of the Norwegian Caledonides. Journal of Petrology 53, 1357–1383.
Brueckner, H.K., 2009. Subduction of continental crust, the origin of post-orogenic granitoids (and anorthosites?) and the evolution of Fennoscandia. Journal of the Geological Society of London 166, 753–762.
Brueckner, H.K., van Roermund, H.L.M., 2004. Dunk tectonics: a multiple subduction/eduction model for the evolution of the Scandinavian Caledonides. Tectonics 23, TC2004.
Butler, J.P., Jamieson, R.A., Steenkamp, H.M., Robinson, P., 2013. Discovery of coesite–eclogite from the Nordøyane UHP domain, Western Gneiss Region, Norway: field relations, metamorphic history, and tectonic significance. Journal of Metamorphic Geology. http://dx.doi.org/10.1111/jmg.12004.
Carswell, D.A., van Roermund, H.L.M., 2005. On multi-phase inclusions associated with microdiamond formation in mantle-derived peridotite lens at Bardane on Fjortoft, west Norway. European Journal of Mineralogy 17, 31–42.
Carswell, D.A., Cuthbert, S.J., Ravna, E.J.K., 1999. Ultrahigh-pressure metamorphism in the Western Gneiss Region of the Norwegian Caledonides. International Geology Review 41, 955–966.
Carswell, D.A., Brueckner, H.K., Cuthbert, S.J., Mehta, K., O'Brien, P.J., 2003a. The timing of stabilisation and exhumation rate for ultra-high pressure rocks in the Western Gneiss Region of Norway. Journal of Metamorphic Geology 21, 601–612.
Carswell, D.A., Tucker, R.D., O'Brien, P.J., Krogh, T.E., 2003b. Coesite micro-inclusions and the U/Pb age of zircons from the Hareidland eclogite in the Western Gneiss Region of Norway. Lithos 67, 181–190.
Carswell, D.A., van Roermund, H.L.M., Wiggers de Vries, D.F., 2006. Scandian ultrahigh-pressure metamorphism of Proterozoic basement rocks on Fjortoft and Otroy, Western Gneiss Region, Norway. International Geology Review 48, 957–977.
Chopin, C., 1984. Coesite and pure pyrope in high-grade blueschists of the Western Alps — a 1st record and some consequences. Contributions to Mineralogy and Petrology 86, 107–118.
Coleman, R.G., Lee, D.E., Beatty, L.B., Brannock, W.W., 1965. Eclogites and eclogites: their differences and similarities. Geological Society of America Bulletin 76, 483–508.
Cuthbert, S.J., Carswell, D.A., Krogh-Ravna, E.J., Wain, A., 2000. Eclogites and eclogites in the Western Gneiss Region, Norwegian Caledonides. Lithos 52, 165–195.
Dobrzhinetskaya, L.F., Eide, E.A., Larsen, R.B., Sturt, B.A., Trønnes, R.G., Smith, D.C., Taylor, W.R., Posukhova, T.V., 1995. Microdiamond in high-grade metamorphic rocks of the Western Gneiss Region, Norway. Geology 23, 597–600.
Engvik, A.K., Andersen, T.B., Wachmann, M., 2007. Inhomogeneous deformation in deeply buried continental crust, an example from the eclogite-facies province of the Western Gneiss Region, Norway. Norwegian Journal of Geology 87, 373–389.
Foreman, R., Andersen, T.B., Wheeler, J., 2005. Eclogite-facies polyphase deformation of the Drosdal eclogite, Western Gneiss Complex, Norway, and implications for exhumation. Tectonophysics 398, 1–32.
Fossen, H., 2010. Extensional tectonics in the North Atlantic Caledonides: a regional view. In: Law, R.D., Butler, R.W.H., Holdsworth, R.E., Krabbendam, M., Strachan, R.A. (Eds.), Continental Tectonics and Mountain Building: The Legacy of Peach and Horne: Geological Society of London Special Publications, 335, pp. 767–793.
Gorbatschev, R., 1985. Precambrian basement of the Scandinavian Caledonides. In: Gee, D.G., Sturt, B.A. (Eds.), The Caledonian Orogen — Scandinavia and Related Areas. J. Wiley & Sons, Chichester, pp. 197–212.
Gordon, S.M., Grove, M., Whitney, D.L., Schmitt, A.K., Teyssier, C., 2009. Fluid–rock interaction in orogenic crust tracked by zircon depth profiling. Geology 37, 735–738.

Gordon, S.M., Bowring, S.A., Whitney, D.L., Miller, R.B., McLean, N., 2010. Time scales of metamorphism, deformation, and crustal melting in a continental arc, North Cascades USA. Geological Society of America Bulletin 122, 1308–1330.
Griffin, W.L., Brueckner, H.K., 1985. REE, Rb–Sr, and Sm–Nd studies of Norwegian eclogites. Chemical Geology 52, 249–291.
Hacker, B.R., 2006. Pressures and temperatures of ultrahigh-pressure metamorphism: implications for UHP tectonics and H_2O in subducting slabs. International Geology Review 48, 1053–1066.
Hacker, B.R., 2007. Ascent of the ultrahigh-pressure Western Gneiss Region, Norway. In: Cloos, M., Carlson, W.D., Gilbert, M.C., Liou, J.G., Sorenson, S.S. (Eds.), Convergent Margin Terranes and Associated Regions: A Tribute to W.G. Ernst: Geological Society of America Special Paper, 419, pp. 171–184.
Hacker, B.R., Gans, P.B., 2005. Continental collisions and the creation of ultrahigh-pressure terranes: petrology and thermochronology of nappes in the central Scandinavian Caledonides. Geological Society of America Bulletin 117, 117–134.
Hacker, B.R., Andersen, T.B., Root, D.B., Mehl, L., Mattinson, J.M., Wooden, J.L., 2003. Exhumation of high-pressure rocks beneath the Solund Basin, Western Gneiss Region of Norway. Journal of Metamorphic Geology 21, 613–629.
Hacker, B.R., Andersen, T.B., Johnston, S., Kylander-Clark, A.R.C., Peterman, E.M., Walsh, E.O., Young, D., 2010. High-temperature deformation during continental-margin subduction and exhumation: the ultrahigh-pressure Western Gneiss Region of Norway. Tectonophysics 480, 149–171.
Hermann, J., 2002. Experimental constraints on phase relations in subducted continental crust. Contributions to Mineralogy and Petrology 143, 219–235.
Hollocher, K., Robinson, P., Terry, M.P., Walsh, E., 2007. Application of major- and trace-element geochemistry to refine U–Pb zircon, and Sm/Nd or Lu/Hf sampling targets for geochronology of HP and UHP eclogites, Western Gneiss Region, Norway. American Mineralogist 92, 1919–1924.
Hoskin, P.W.O., Schaltegger, U., 2003. The composition of zircon and igneous and metamorphic petrogenesis. In: Hanchar, J.M., Hoskin, P.W.O. (Eds.), Zircon: Reviews in Mineralogy and Geochemistry, 53, pp. 27–62.
Johnson, D.M., Hooper, P.R., Conrey, R.M., 1999. XRF analysis of rocks and minerals for major and trace elements on a single low dilution Li-tetraborate fused bead. Advances in X-ray Analysis 41, 843–867.
Johnston, S., Hacker, B.R., Ducea, M.N., 2007. Exhumation of ultrahigh-pressure rocks beneath the Hornelen segment of the Nordfjord-Sogn Detachment Zone, western Norway. Geological Society of America Bulletin 119, 1232–1248.
Krogh, T., Kwok, Y., Robinson, P., Terry, M.P., 2004. U–Pb constraints on the subduction–extension interval in the Averøya–Nordøyane area, Western Gneiss Region, Norway. Goldschmidt Conference.European Association for Geochemistry, Copenhagen, Denmark.
Krogh, T.E., Kamo, S.L., Robinson, P., Terry, M.P., Kwok, K., 2011. U–Pb zircon geochronology of eclogites from the Scandian Orogen, northern Western Gneiss Region, Norway: 14–20 million years between eclogite crystallization and return to amphibolite-facies conditions. Canadian Journal of Earth Sciences 48. http://dx.doi.org/10.1139/E10-076.
Kullerud, L., Tørudbakken, B., Ilebekk, S., 1986. A compilation of radiometric age determinations from the Western Gneiss Region, south Norway. Norges Geologiske Undersøkelse 406, 17–42.
Kylander-Clark, A.R.C., Hacker, B.R., Johnson, C.M., Beard, B.L., Mahlen, N.J., Lapen, T.J., 2007. Coupled Lu–Hf and Sm–Nd geochronology constrains prograde and exhumation histories of high- and ultrahigh-pressure eclogites from western Norway. Chemical Geology 242, 137–154.
Kylander-Clark, A.R.C., Hacker, B.R., Mattinson, J.M., 2008. Slow exhumation of UHP terranes: titanite and rutile ages of the Western Gneiss Region, Norway. Earth and Planetary Science Letters 272, 531–540.
Kylander-Clark, A.R.C., Hacker, B.R., Johnson, C.M., Beard, B.L., Mahlen, N.J., 2009. Slow subduction of a thick ultrahigh-pressure terrane. Tectonics 28. http://dx.doi.org/10.1029/2007TC002251.
Kylander-Clark, A.R.C., Hacker, B.R., Cottle, J., in press. Laser-ablation split-stream ICP petrochronology. Chemical Geology.
Labrousse, L., Prouteau, G., Ganzhorn, A.-C., 2011. Continental exhumation triggered by partial melting at ultrahigh pressure. Geology 39, 1171–1174.
Lang, H.J., Gilotti, J.A., 2007. Partial melting of metapelites at ultrahigh-pressure conditions, Greenland Caledonides. Journal of Metamorphic Geology 25, 129–147.
Liou, J.G., Hacker, B.R., Zhang, R.Y., 2000. Into the forbidden zone. Science 287, 1215–1216.
Liu, F.L., Robinson, P.T., Liu, P.H., 2012. Multiple partial melting events in the Sulu UHP terrane: zircon U–Pb dating of granitic leucosomes within amphibolite and gneiss. Journal of Metamorphic Geology 30, 887–906.
Ludwig, K.R., 2003. Isoplot 3.00: A geochronological toolkit for Microsoft Excel. Berkeley Geochronology Center, Special Publication 4 [70 pp.].
Mørk, M.B.E., Mearns, E.W., 1986. Sm–Nd isotopic systematics of a gabbro–eclogite transition. Lithos 19, 255–267.
Patiño Douce, A.E., McCarthy, T.C., 1998. Melting of crustal rocks during continental collision and subduction. In: Hacker, B.R., Liou, J.G. (Eds.), When Continents Collide: Geodynamics and Geochemistry of Ultrahigh-pressure Rocks. Kluwer Academic, pp. 27–55.
Prouteau, G., Scaillet, B., Pichavant, M., Maury, R., 2001. Evidence for mantle metasomatism by hydrous silicic melts derived from subducted oceanic crust. Nature 410, 197–200.
Ravna, E.J.K., Terry, M.P., 2004. Geothermobarometry of phengite–kyanite–quartz/coesite eclogites. Journal of Metamorphic Geology 22, 579–592.
Root, D.B., Hacker, B.R., Mattinson, J.M., Wooden, J.L., 2004. Zircon geochronology and ca. 400 Ma exhumation of Norwegian ultrahigh-pressure rocks: an ion microprobe and chemical abrasion study. Earth and Planetary Science Letters 228, 325–341.
Root, D.B., Hacker, B.R., Gans, P.B., Ducea, M.N., Eide, E.A., Mosenfelder, J.L., 2005. Discrete ultrahigh-pressure domains in the Western Gneiss Region, Norway: implications for formation and exhumation. Journal of Metamorphic Geology 23, 45–61.
Rosenberg, C.L., Handy, M.R., 2005. Experimental deformation of partially melted granite revisited: implications for the continental crust. Journal of Metamorphic Geology 23, 19–28.
Rubatto, D., 2002. Zircon trace element geochemistry: distribution coefficients and the link between U–Pb ages and metamorphism. Chemical Geology 184, 123–138.
Rubatto, D., Hermann, J., 2001. Exhumation as fast as subduction? Geology 29, 3–6.
Scambelluri, M., Pettke, T., van Roermund, H.L.M., 2008. Majoritic garnets monitor deep subduction fluid flow and mantle dynamics. Geology 36, 59–62.
Schärer, U., Labrousse, L., 2003. Dating the exhumation of UHP rocks and associated crustal melting in the Norwegian Caledonides. Contributions to Mineralogy and Petrology 144, 758–770.
Skår, O., Pedersen, R.B., 2003. Relations between granitoid magmatism and migmatization: U–Pb geochronological evidence from the Western Gneiss Complex, Norway. Journal of the Geological Society 160, 935–946.
Smith, D.C., 1984. Coesite in clinopyroxene in the Caledonides and its implications for geodynamics. Nature 310, 641–644.
Smith, D.C., Godard, G., 2013. A Raman spectroscopic study of diamond and disordered sp^3-carbon in the coesite-bearing Straumen eclogite pod, Norway. Journal of Metamorphic Geology 31, 19–33.
Spencer, K., Hacker, B.R., Kylander-Clark, A.R.C., Andersen, T.B., Cottle, J.M., Stearns, M.A., Poletti, J.E., Seward, G.G.E., in press. Campaign-style titanite U–Pb dating by ICP: implications for crustal flow, phase transformations and titanite closure. Chemical Geology.
Spengler, D., Brueckner, H.K., van Roermund, H.L.M., et al., 2009. Long-lived, cold burial of Baltica to 200 km depth. Earth and Planetary Science Letters 281, 27–35.
Terry, M.P., Robinson, P., 2003. Evolution of amphibolite-facies structural features and boundary conditions for deformation during exhumation of high- and ultrahigh-pressure rocks, Nordoyane, Western Gneiss Region, Norway. Tectonics 22. http://dx.doi.org/10.1029/2001TC001349.
Terry, M.P., Robinson, P., 2004. Geometry of eclogite-facies structural features: implications for production and exhumation of UHP and HP rocks, Western Gneiss Region, Norway. Tectonics 23. http://dx.doi.org/10.1029/2002TC001401.
Terry, M.P., Robinson, P., Ravna, E.J.K., 2000a. Kyanite eclogite thermobarometry and evidence for thrusting of UHP over HP metamorphic rocks, Nordoyane, Western Gneiss Region, Norway. American Mineralogist 85, 1637–1650.
Terry, M.P., Robinson, P., Hamilton, M.A., Jercinovic, M.J., 2000b. Monazite geochronology of UHP and HP metamorphism, deformation, and exhumation, Nordøyane, Western Gneiss Region, Norway. American Mineralogist 85, 1651–1664.
Tucker, R.D., Boyd, R., Barnes, S.J., 1990. A U–Pb zircon age for the Rana intrusion, N Norway — new evidence of basic magmatism in the Scandinavian Caledonides in early Silurian time. Norsk Geologisk Tidsskrift 70, 229–239.
van Roermund, H.L.M., Drury, M.R., Barnhoorn, A., De Ronde, A., 2001. Relict majoritic garnet microstructures from ultra-deep orogenic peridotites in western Norway. Journal of Petrology 42, 117–130.
van Roermund, H.L.M., Carswell, D.A., Drury, M.R., Heijboer, T.C., 2002. Microdiamonds in a megacrystic garnet websterite pod from Bardane on the island of Fjortoft, western Norway: evidence for diamond formation in mantle rocks during deep continental subduction. Geology 30, 959–962.
Vorhies, S.H., Ague, J.J., Schmitt, A.K., 2013. Zircon growth and recrystallization during progressive metamorphism, Barrovian zones, Scotland. American Mineralogist 98, 219–230.
Vrijmoed, J.C., van Roermund, H.L.M., Davies, G.R., 2006. Evidence for diamond-grade ultra-high pressure metamorphism and fluid interaction in the Svartbarget Fe–Ti garnet peridotite–websterite body, Western Gneiss Region, Norway. Mineralogy and Petrology 88, 381–405.
Vrijmoed, J.C., Podladchikov, Y., Andersen, T.B., Hartz, E., 2009. An alternative model for ultrahigh pressure in the Svartberget Fe–Ti garnet–peridotite, Western Gneiss Region, Norway. European Journal of Mineralogy 21, 1119–1133.
Wain, A., 1997. New evidence for coesite in eclogite and gneisses: defining an ultrahigh-pressure province in the Western Gneiss region of Norway. Geology 25, 927–930.
Wain, A., Waters, D., Jephcoat, A., Olijynk, H., 2000. The high-pressure to ultrahigh-pressure eclogite transition in the Western Gneiss Region, Norway. European Journal of Mineralogy 12, 667–687.
Wain, A.L., Waters, D.J., Austrheim, H., 2001. Metastability of granulites and processes of eclogitisation in the UHP region of western Norway. Journal of Metamorphic Geology 19, 607–623.
Wallis, S., Tsuboi, M., Suzuki, K., Fanning, M., Jiang, L., Tanaka, T., 2005. Role of partial melting in the evolution of the Sulu (eastern China) ultrahigh-pressure terrane. Geology 33, 129–132.
Walsh, E.O., Hacker, B.R., 2004. The fate of subducted continental margins: two-stage exhumation of the high-pressure to ultrahigh-pressure Western Gneiss Region, Norway. Journal of Metamorphic Geology 22, 671–687.
Walsh, E.O., Hacker, B.R., Gans, P.B., Grove, M., Gehrels, G., 2007. Protolith ages and exhumation histories of (ultra)high-pressure rocks across the Western Gneiss Region, Norway. Geological Society of America Bulletin 119, 289–301.
Whitney, D.L., Teyssier, C., Fayon, A.K., 2004. Isothermal decompression, partial melting, and the exhumation of deep continental crust. In: Grocott, J., Tikoff, B., McCaffrey, K.J.W., Taylor, G. (Eds.), Vertical Coupling and Decoupling in the Lithosphere: Geological Society of London Special Publication, vol. 227, pp. 313–326.
Whitney, D.L., Teyssier, C., Rey, P.F., 2009. The consequences of crustal melting in continental subduction. Lithosphere 1, 323–327.
Zhang, L., Zhong, Z., Zhang, H., Sun, W., Xiang, H., 2009. The formation of foliated (garnet-bearing granites in the Tongbai–Dabie orogenic belt: partial melting of subducted continental crust during exhumation. Journal of Metamorphic Geology 27, 789–803.